Sustainable Chemistry and Pharmacy 45 (2025) 102037

Contents lists available at ScienceDirect

Sustainable Chemistry and Pharmacy

journal homepage: www.elsevier.com/locate/scp

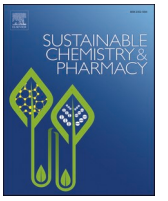

Molecular landscape of therapeutic deep eutectic systems selective toxicity towards colorectal cancer

Filipe Oliveira [a], Joana Pinto [b,c], Filipa Amaro [b,c], Joana Pereira [a], Inês Ferreira [a], Mário S. Diniz [d,e], Paula Guedes de Pinho [b,c], Ana Rita C. Duarte [a,*]

[a] LAQV/REQUIMTE, Department of Chemistry, NOVA School of Science and Technology, 2829-516, Caparica, Portugal
[b] Associate Laboratory i4HB – Institute for Health and Bioeconomy, University of Porto, 4050-313, Porto, Portugal
[c] UCIBIO – Applied Molecular Biosciences Unit, Laboratory of Toxicology, Department of Biological Sciences, Faculty of Pharmacy, University of Porto, 4050-313, Porto, Portugal
[d] UCIBIO – Applied Molecular Biosciences Unit, Department of Chemistry, NOVA School of Science and Technology, 2829-516, Caparica, Portugal
[e] Associate Laboratory I4HB – Institute for Health and Bioeconomy, NOVA School of Science and Technology, 2819-516, Caparica, Portugal

ARTICLE INFO

Handling Editor: Fabio Aricò

Keywords:
Green chemistry
Therapeutic deep eutectic systems
Anticancer
Metabolomics
In vivo toxicity

ABSTRACT

The foremost modern medicine challenges, such as cancer's high mortality rates, have emphasized the growing need for improved therapeutic agents. Following eutectic systems spotlight due to their remarkable physicochemical and biological properties, while mostly in compliance with the Green Chemistry Principles and sustainability metrics as the Sustainable Development Goals (SDG) from United Nations, we aimed to push forward their understanding as anticancer agents. Considering therapeutic deep eutectic systems (THEDES) promising reports of anticancer activity towards colorectal cancer (CRC) cells, we sought to fill the knowledge gap on these eutectics impact on these cancer cells molecular landscape. For that, an integrated approach was used to study how combining a terpene – as menthol (Me), thymol (Thy), perillyl alcohol (POH) and limonene (Lim) – with ibuprofen (Ibu) as a THEDES, affects permeability, cellular transport, cell viability, reactive oxygen species (ROS), cell metabolome and systemic toxicity. THEDES exposure resulted in increased Ibu cellular uptake, depletion of ROS, and cell dead induction via apoptosis. Moreover, CRC cells experienced alterations in their metabolite landscape with deleterious effects on essential metabolic pathways, such as lipid and anaerobic glycolysis energy production pathways. Furthermore, non-relevant systemic toxicity of these THEDES, within the range of concentrations tested, was observed. These findings underscore THEDES potential as selective anticancer agents, while offering a promising path for the development of therapeutics aligned with the sustainability metrics.

1. Introduction

The classical definition of a deep eutectic system (DES) is a mixture of two compounds, which, when combined in a particular molar ratio, exhibit a lower melting temperature than its initial pure components. This phenomenon may be attributed to hydrogen bonding between a hydrogen bond donor and a hydrogen bond acceptor, alongside with other intermolecular interactions such as electrostatic van der Waals forces (Hansen et al., 2021; Zhang et al., 2012). Abbot and coworkers reported the preparation of a liquid system

* Corresponding author.
E-mail address: aduarte@fct.unl.pt (A.R.C. Duarte).

https://doi.org/10.1016/j.scp.2025.102037
Received 13 March 2025; Received in revised form 17 April 2025; Accepted 23 April 2025
Available online 1 May 2025

combining urea and a quaternary ammonium salt and demonstrated that sustainable, biodegradable and highly flexible mixtures could be produced from readily available components and tailored to specific applications, while mostly in compliance with the Principles of Green Chemistry and sustainability regarding United Nations's SDG from the 2030 agenda for sustainable development (Abbott et al., 2003; Anastas and Warner, 1998; United Nations, 2016). This paved the way to a number of reports on eutectics for different applications, namely in the biomedical field, with promising bioactivities as anticancer agents, bioavailability enhancers, antimicrobial and antibiofilm agents, and also as wound healing enhancers (Nakaweh et al., 2024; Zainal-Abidin et al., 2019; Oliveira et al., 2023; Valente et al., 2023; Wikene et al., 2017; Radošević et al., 2018; Silva et al., 2020, 2021; Zakrewsky et al., 2016; Mbous et al., 2017, 2020). When an active pharmaceutical ingredient (API) is part of the eutectic composition, the system is thereafter designated by THEDES. In this way, the fundaments of eutecticity have been applied in attempts to overcome the outmost challenges of modern medicine such as the pursuit for therapeutics with more selectiveness towards cancer.

Cancer remains as the second leading cause of death worldwide and, in particular, colorectal cancer (CRC) is among the most incident and also the most mortal ones (Bray et al., 2024; Sung et al., 2025). CRC is a long-term developing disease which can often take 5–10 years for the patient to feel symptoms (Hnatyszyn et al., 2019; Baars et al., 2012). CRC carcinogenesis highly relies on inflammation and angiogenesis for providing the essential nutrients for its unregulated cell proliferation. Thus, chronic inflammatory states, such as inflammatory bowel disease, represent a severe risk factor for CRC development (Coussens and Werb, 2002; Apple et al., 2016). Besides, CRC carcinogenesis may be induced by the human gut microbiome via a variety of different mechanisms, including microbial-derived factors such as metabolites or genotoxins, bacterial invasion, and/or activation of immune response (Ogunrinola et al., 2020; Cheng et al., 2020). Hence CRC multifactor carcinogenesis results in the need for a therapeutic agent able to cope with a very heterogenic therapeutic profile.

Nowadays, its conventional treatment mostly encompasses surgery followed by chemotherapy with fluorouracil (5-FU), leucovorin and oxaliplatin (Kumar et al., 2023). However, metastatic CRC can be resistant to such conventional therapeutics (Aylaz et al., 2021). For this reason there have been efforts to develop not only optimized strategies for earlier diagnosis and watch-and-wait strategies, but also therapeutic agents that have higher selectiveness towards its cancer targets (Ladabaum et al., 2020; Byun and Koom, 2023).

Furthermore, considering sustainability metrics as the environmental factor (E-factor) – which relates the mass of waste produced per mass of product formed – it has been reported that its values vary significantly across industries, with the pharmaceutical industry standing out with the highest values, ranging from 25 to 100 kg of waste per kg of product (bulk chemicals <1–5 kg and fine chemicals 5–50 kg) (Lam et al., 2019; Sheldon, 2017). Hence, in addition to pursuing highly selective therapeutic agents, efforts should also focus on designing and implementing more efficient processes that minimize waste generation in the pharmaceutical industry.

There have been several reports on eutectic formulations with promising anticancer action. Hayyan and coworkers have reported an interesting cytotoxic profile of different ammonium-based eutectic systems towards several cancer cell lines, such as breast cancer (MCF-7), prostate cancer (PC3), malignant melanoma (A375), liver hepatocellular (HepG2), CRC (HT29) and carcinoma-derived oral keratinocytes (H413) (Hayyan et al., 2015). Likewise, in another study, damages on cancer cell membrane as a consequence of eutectic system exposure were reported, using combinations of choline chloride with glucose and fructose, and N,N-diethylethanol ammonium chloride and triethylene glycol (Mbous et al., 2017, 2020). Nevertheless, despite the evidence on eutectic systems anticancer therapeutic role, a better understanding of these systems specific impact on living systems is necessary.

Considering the previously reported work on THEDES combining different terpenes (Me, Thy, POH, and Lim) with Ibu (Silva et al., 2020, 2021; Pereira et al., 2019, 2022), this work aims to provide a broader understanding of how this anticancer action occurs, namely using a metabolomic approach, to provide direct insights into the cellular biochemical landscape upon THEDES exposure (Wishart, 2016). Furthermore, a preliminary indication on THEDES systemic toxicity using a zebrafish animal model was assessed, pushing forward the establishment of eutectics as a sustainable alternative or complementary therapeutic agent for CRC.

2. Materials and methods

2.1. THEDES preparation

THEDES were prepared using racemic menthol (Me, ref. W266507-1000, Sigma, USA), thymol (Thy, ref. T0501, Sigma, USA), (S)-(−)-perillyl alcohol (POH, ref. W266418, Sigma, USA), S-Limone (Lim, ref. 218367 Sigma, USA), and ibuprofen (Ibu, ref. B20989, Alfa Aesar, USA). Different eutectic mixtures using these individual compounds were prepared, such as Me:Ibu (3:1), Thy:Ibu (3:1), POH:Ibu (3:1), POH:Ibu (8:1), Lim:Ibu (4:1) and Lim:Ibu (8:1) as previously reported (Silva et al., 2020, 2021; Pereira et al., 2019; Aroso et al., 2015). THEDES were prepared by mixing and heating both components at 40 °C, under constant stirring, until a clear liquid was observed. Afterward, THEDES were left to cool down at room temperature (RT). THEDES were prepared right before each assay or stored at −20 °C.

2.2. Permeability assessment using a synthetic membrane

Ibu's permeability was assessed using glass diffusion Franz cells (PermeGear, USA) with an 8 mL receptor compartment and an effective mass transfer area of 1 cm^2. A polyethersulphone (PES-U) hydrophilic membrane (15406–25-N, Sartorius Stedim Biotech, Germany) was used. Ibu in powder form or THEDES were added to the donor compartment, along with 2 mL of PBS, obtaining a final concentration of 2.5–3 mg/mL. Subsequently, 400 μL were retrieved from the receptor compartment at different time points (10 min and hourly from 1 to 8 h) and replaced with the same volume of fresh PBS. The experience was conducted at 37 °C under constant stirring (200 rpm) using a magnetic bar for eliminating the boundary layer effect. At least three replicates of the experience were

performed. The quantification of the amount of diffused Ibu was performed by HPLC, as previously reported for the same THEDES (Silva et al., 2020, 2021; Pereira et al., 2019).

The cumulative mass of Ibu diffused to the receptor compartment was determined considering the replacement of the aliquots with fresh PBS and the dilution associated with it. Ibu's permeability (P) and diffusion coefficient were determined following the equations described elsewhere (Duarte et al., 2017; Ascar et al., 2013; Silva et al., 2014; Chu et al., 2004).

2.3. Bioactivity assessment

2.3.1. Cell culture

Caco-2 and HT29 are immortalized human colorectal adenocarcinoma cell lines herein used as 2D *in vitro* cell models for colorectal cancer. They were both obtained from the Deutsche Sammlung von Mikroorganismen und Zellkulturen (DSMZ, Germany). And both subcultured in Gibco Roswell Park Memorial Institute (RPMI, Corning, United States) 1640 medium with phenol red, supplemented with 10 % (v/v) of heat-inactivated fetal bovine serum (FBS, Corning, United States) and 1 % (v/v) penincilin-strepmycin (PS, Corning, United States). Cell culture was maintained at 37 °C with 5 % CO_2 in a humidified incubator, and routinely grown as a monolayer in 75 cm^2 cell culture flasks.

2.3.2. Transwell permeability assessment

The permeability of Ibu in power and in THEDES form through intestine cells was measured using the transwell permeability assay. For that, a continuous cell layer of heterogeneous human epithelial colorectal adenocarcinoma cells (Caco-2) (ACC 169, DSMZ, Braunschweig, Germany) was used (Sambuy et al., 2005). Cells were seeded in a transwell cell culture insert (diameter = 6.4 mm; pore size = 0.4 μm; growth area = 0.3 cm^2 - ref. 353095, Falcon, Corning, USA) in a 24 well plate at a 1.61×10^5 cells/ml concentration for 25 days, to allow cells to fully differentiate. The monolayer integrity was verified by measuring the transepithelial electrical resistance (TEER). Ibu transport from the apical to the basolateral chamber was performed using PBS as physiological-like medium. Ibu in powder form or THEDES were prepared in PBS obtaining a final concentration of 0.1–0.5 mg/mL. For that, 250 μL of the samples diluted in PBS or PBS alone (control) were added to the apical chamber, and 750 μL of PBS was placed in the basolateral chamber. Samples of 400 μL were retrieved from the basolateral chamber in the first 30 min, and then every hour until 6 h, and replaced by the same amount of fresh PBS. These permeability experiments were conducted in triplicate at 37 °C in a humified atmosphere with 5 % CO_2. The determination of Ibu diffused was performed by HPLC, as described elsewhere (Silva et al., 2020, 2021). The estimated apparent permeability (Papp) was calculated following the mathematical approach reported elsewhere (Santos et al., 2023).

2.3.3. Intracellular reactive oxygen species (ROS) production

THEDES effect on ROS production in CRC cells was assessed using the HT29 cell model as previously reported (Pereira et al., 2022). Briefly, cells were seeded in a 24-well plate at a density of 1.52×10^5 cells/mL. After 24 h, cell culture was exposed to the respective EC_{50} of each THEDES, particularly 4.30 mM for Me:Ibu (3:1), 0.30 mM for Thy:Ibu (3:1), 1.32 mM for POH:Ibu (3:1), 1.37 mM for POH:Ibu (8:1), 2.39 mM for Lim:Ibu (4:1) and 1.14 mM for Lim:Ibu (8:1), and their corresponding individual compounds diluted in culture medium or just culture medium for 1 h. Cells with just culture medium worked as negative control. Thereafter, the culture media was removed and cells were washed twice with PBS. Finally, for ROS quantification, 600 μL of 2′,7′-Dichlorofluorescein diacetate (DCFH-DA) in a 25 μM concentration were added to each well and left for 1 h. The resulting fluorescence was measured in a microplate reader (HH35L2019044, Victor Nivo 3S, PerkinElmer, USA) applying an excitation wavelength of 480 nm and an emission wavelength of 530 nm. At least three replicates were performed in triplicate.

2.3.4. Lactate dehydrogenase (LDH) release

The assessment of THEDES influence on membrane integrity was evaluated through the release of LDH to the extracellular media. To achieve that, the LDH-Cytox™ Assay Kit (426401, Biolegend, USA) was used according to manufacturer's instructions with some modifications to the protocol as previously reported (Pereira et al., 2022). HT29 cells were exposed to Thy:Ibu (3:1), POH:Ibu (3:1), POH:Ibu (8:1), Lim:Ibu (4:1) and Lim:Ibu (8:1), using six 2-fold serial dilutions. All dilutions were performed in triplicate. The resulting absorbance was measured at 490 nm, in a microplate reader (HH35L2019044, Victor Nivo 3S, PerkinElmer, USA). The results are expressed in percentage of LDH released in comparison to the "High Control" and "Low Control", determined using Equation (4):

$$\text{LDH release } (\%) = \frac{\text{Abs(tested substanceTHEDES)} - \text{Abs(Low Control)}}{\text{Abs(High Control)} - \text{Abs(Low Control)}} \times 100 \quad (1)$$

2.3.5. Caspase-3 activity

THEDES potential to activate apoptosis via the caspase-3 pathway was assessed using HT29 cells as previously reported (Pereira et al., 2022). Briefly, cells were seeded in 24-well plates at a density of 1.52×10^5 cells/mL and left incubating for 24 h. Thereafter, cells were exposed to THEDES previously described antiproliferative EC_{50}, as 4.30 mM for Me:Ibu (3:1), 0.30 mM for Thy:Ibu (3:1), 1.32 mM for POH:Ibu (3:1), 1.37 mM for POH:Ibu (8:1), 2.39 mM for Lim:Ibu (4:1) and 1.14 mM for Lim:Ibu (8:1), and their individual compounds diluted in culture media or just culture medium working as negative control for 24 h. Staining of live and death cells was achieved using NucView®488 and Mito-ViewTM633 Apoptosis Assay Kit (Biotium, USA) according to manufacturer's instructions. The resulting fluorescence was observed using an inverted optical microscope (Zeiss, Axio Vert A1, Germany) with a Colibri 7 (Zeiss, Germany) light source, and micrographs were recorded using ZEN 3.5 (blue edition) software (Zeiss, Germany). Cells were subjected to

an excitation and emission wavelengths of 631 nm and 650 nm for MitoViewTM633, and an excitation wavelength of 500 nm and emission wavelength of 520 nm for NucView®488.

2.3.6. Statistical analysis

Statistical analysis of the resulting data was carried out using GraphPad Prism 9.0 (GraphPad Software, USA). All data are expressed as mean ± standard deviation (SD). Significant differences were calculated by comparing the control with the different compounds, where P-values smaller than 0.05 were considered statistically significant (confidence interval of 95 %). Statistical differences are represented by different symbols, as *p ≤ 0.05, **p ≤ 0.01, ***p ≤ 0.001 and ****p ≤ 0.0001. To assess significant statistical differences, first the normal distribution of results was tested using the Shapiro-Wilk test. When the results followed a normal distribution, One-Way ANOVA was used to perform the comparisons following Dunnett or Tukey multiple comparison test. When results did not follow a normal distribution, Kruskal-Wallis test was performed.

2.4. Metabolomic assessment

2.4.1. Extracellular metabolome collection

HT29 cells were seeded at a density of 1.5×10^5 cells/mL in 24 well cell culture plates (CLS3526, Corning, USA). After 24 h cells were incubated with THEDES diluted in culture medium using the corresponding antiproliferative EC_{50} previously described, as 4.30 mM for Me:Ibu (3:1), 0.30 mM for Thy:Ibu (3:1), 1.32 mM for POH:Ibu (3:1), 1.37 mM for POH:Ibu (8:1), 2.39 mM for Lim:Ibu (4:1) and 1.14 mM for Lim:Ibu (8:1) or just culture medium (Silva et al., 2020, 2021; Pereira et al., 2019). Cells incubated with only supplemented culture medium were considered as control, and supplemented culture medium alone considered as blank. All tested conditions were incubated at 37 °C with 5 % CO_2 for 24 h. The assay incubation period was chosen so that cells are experiencing their exponential growth phase and, therefore, THEDES exposure could express an antiproliferative effect assessment. At the end of the incubation period, control and exposure media were collected, centrifuged at 2000 g for 5 min at 4 °C, and the supernatant was stored at −80 °C until exometabolome analysis. At least eight independent experiments from eight different consecutive cell subculturing steps were herein used, considering one sample for each condition under study. To assess the analytical reproducibility of the experiment, a pool of the extracellular media of all samples was also prepared and divided into aliquots to be used as quality control (QCs).

2.4.2. Intracellular metabolome extraction

The adherent cells from the previously described procedure were collected for endometabolome analysis. Briefly, cell monolayers were washed twice with a saline solution (0.9 % NaCl), and 1.5 mL cold (−20 °C) methanol:H_2O (80:20 v/v) was added to stop cellular metabolism. Then, cells were scrapped from the 24 well cell culture plates (CLS3526, Corning, USA) and transferred to microtubes. Thereafter, cells were sonicated with the microtubes always in ice for 3 cycles of 30 s at 23 kHz with 10 μM of amplitude relying on an exponential probe, with 30 s in ice between each sonication cycle. Finally, cells were centrifuged at 3000 g for 10 min at 4 °C and the supernatant was collected and stored at −80 °C. Similarly to what was described in the previous extracellular metabolome collection step, at least five independent experiments from eight different consecutive cell subculturing steps were herein used, considering one sample for each condition under study. Also, to assess the analytical reproducibility of the experiment, a pool of the intracellular metabolome extracts of all samples was also prepared and divided into aliquots to be used as QCs.

2.4.3. Sample preparation for analysis of intracellular and extracellular metabolites

The preparation of intracellular extracts for analysis started by thawing slowly at room temperature the frozen samples and controls. Thereafter, 5 μL of desmosterol (1 mg/mL) (internal standard) was added to 1 mL of each sample in a glass vial. Samples were vortexed for 1 min and evaporated under a constant gentle nitrogen stream until completely dried. Then, 50 μL of methoxyamine (15 mg/mL methoxyamine hydrochloride in pyridine) was added to each sample, followed by incubation for 6 min at 70 °C. Then, 100 μL of N,O-Bis(trimethylsilyl)trifluoroacetamide (BSTFA) with 1 % trimethylchlorosilane (TMS) were added and samples were incubated for 60 min at room temperature. The derivatized extracts were placed in glass vials and 2 μL of each was randomly injected in the GC-MS at a split mode ratio of 1:20. QCs were run under the same conditions on every 5 samples.

For analysis of the extracellular metabolites, stored culture media were thawed slowly on ice. Then, 2 mL of each sample was transferred to a 10 mL glass vial with 47 μL of the derivatizing agent (O-(2,3,4,5,6-pentafluorobenzyl) hydroxylamine, 40 g/L). The extraction of volatile carbonyl compounds (aldehydes and ketones) was performed through headspace solid-phase microextraction (HS-SPME) with a polydimethylsiloxane/divinylbenzene (PDMS/DVB) fiber in a Bruker CTC PAL-xt autosampler (Bruker Daltonics, Bremen, Germany). First, the samples were incubated for 6 min at 62 °C, followed by volatile extraction for 51 min at 62 °C, under continuous stirring (250 rpm) (Araújo et al., 2018). All samples were randomly injected, and the QCs were run under the same conditions on every 5 samples.

2.4.4. GC-MS analytical conditions

The analysis of intracellular and extracellular metabolites was performed on a 436-GC system coupled to an EVOQ Triple Quadrupole (TQ) mass detector (Bruker Daltonics, Bremen, Germany) equipped with a Bruker CTC PAL-xt autosampler (Bruker Daltonics, Bremen, Germany) and a Bruker MS workstation software (version 8.2). The chromatographic separation was performed in a fused silica capillary column (Rxi-5Sil MS, 30 m × 0.25 mm × 0.25 μm) from RESTEK Corporation (Bellefonte, PA, USA) with Helium C-60 (Gasin, Leça da Palmeira, Portugal) used as carrier gas at a constant flow rate of 1.0 mL/min. The GC injector temperature was 250 °C.

For intracellular analysis, the oven temperature was fixed at 70 °C for 2 min, increasing to 250 °C (rate 15 °C/min) and held for 2 min, followed by an increase to 300 °C (rate 10 °C/min) and held for 5 min. For extracellular analysis, the oven temperature was defined at 40 °C for 1 min, increasing to 250 °C (rate 5 °C/min), held for 2 min, followed by an increase to 300 °C (rate 5 °C/min) and held for 1 min. The MS detector was operated in electron ionization mode (EI) at 70 eV. The manifold, ion source, and transfer line temperatures were 40 °C, 270 °C, and 260 °C, respectively. The data acquisition was performed in full scan mode considering a mass range of 50–1000 *m/z* (500 scan time) for intracellular extracts, and a mass range of 40–500 *m/z* (500 ms scan time) for extracellular media.

2.4.5. Metabolite annotation and GC-MS data pre-processing

The annotation of metabolites was conducted by comparing the mass spectra of each peak in intracellular and extracellular samples with the mass spectra present in the National Institute of Standards and Technology (NIST 14) database. When commercially available, the identification of metabolites was confirmed by the analysis of standard compounds under the same GC-MS conditions.

The GC-MS data was converted to netcdf format to be pre-processed in the MZmine 2.53 software (Pluskal et al., 2010). The pre-processing steps included filtering, peak detection, chromatogram deconvolution, alignment, duplicate peak filter and gap filling. The parameters used for preprocessing of intracellular data were: RT range 4.90–26.02 min; *m/z* range 50–600; MS data noise level 1×10^5; *m/z* tolerance 0.2; chromatogram baseline level 1×10^4; and peak duration range 0.02–0.5 min. For pre-processing of extracellular data, the parameters were: RT range 14.5–49.0 min; *m/z* range 40–500; MS data noise level 1×10^4; *m/z* tolerance 0.1; chromatogram baseline level 5×10^4; peak duration range 0.02–0.5 min. Contaminants from the chromatographic column, fiber and THEDES were removed from the final matrix (Lima et al., 2018a, 2018b).

2.4.6. Statistical analyses

Firstly, intracellular and extracellular data were normalized by the total area (TA) of the chromatogram and scaled to Pareto. Then, multivariate analysis was performed in MetaboAnalyst 5.0 Pang et al., 2021[46]. Principal component analysis (PCA) was applied to identify major trends in the intracellular and extracellular data and check the analytical reproducibility with QCs. Afterward, partial least squares discriminant analysis (PLS-DA) was performed to assess the ability of intracellular and extracellular metabolites to discriminate between controls and cells treated with THEDES. Metabolites with variable importance to the projection (VIP) in PLS-DA higher than 1 were considered relevant for class discrimination and their statistical significance was assessed by univariate analysis (Mann–Whitney test) in GraphPad Prism 9.0 (GraphPad Software, USA). The metabolites were considered significantly different for *p*-values below 0.05. Finally, the effect size of each significantly altered metabolite was computed as described elsewhere (Berben et al., 2012). The potentially affected metabolic pathways were interpreted using the KEGG and SMPDB databases (Kanehisa et al., 2023; Jewison et al., 2014).

2.5. In vivo toxicity assessment

2.5.1. Animal model and compounds administration

For the *in vivo* toxicity assessment, a zebrafish (*Danio rerio*), obtained from a commercial supplier (Mil Aquários, Portugal), was used as vertebrate model. The animals were acclimated to laboratory conditions at 25 °C for at least 48 h. Thereafter, they were maintained in a 100 L glass aquarium with a closed-circuit system of filtered de-chlorinated tap water, with pH 7.2 ± 0.1 at 20 ± 1 °C, and subject to a photoperiod of 12 h light and 12 h dark, as well as continuous aeration (>6 mg O_2/L). Subsequently, adult fish (n = 5) were randomly selected independently of the sex, since it was not possible to distinguish gender only by external observation. These selected zebrafish were subjected to 10 μL intraperitoneal injections (IP) of either THEDES, or positive and negative controls. The animals were injected with THEDES antiproliferative EC_{50} previously described, as 4.30 mM for Me:Ibu (3:1), 0.30 mM for Thy:Ibu (3:1), 1.32 mM for POH:Ibu (3:1), 1.37 mM for POH:Ibu (8:1), 2.39 mM for Lim:Ibu (4:1) and 1.14 mM for Lim:Ibu (8:1), 5-FU (positive control) (ref. F6627, Sigma, USA) or just culture medium (negative control) (Silva et al., 2020, 2021; Pereira et al., 2019). After IP, the animals were maintained in separate 1.5 L polystyrene aquariums, using the same conditions previously described, and fed every two days with commercial flakes (Tetra brand, USA). The animals were euthanized 96 h after IP by immediate freezing. Afterward, they were weighed and stored at −80 °C until further processing.

All experimental protocols were approved by the FCT ethical committee (CE-FCT-011-2023), meeting the ethical guidelines of the country (Portugal) and complying with EU legislation for animal experimentation (e.g. Directive, 2010/63/EU for animal experimentation and Portuguese Decree-Law 113/2013'on Protection of Animals for Scientific Purposes'). All procedures followed the international guidelines (e.g. the 3 Rs principle of animal welfare) and results reported following the ARRIVE (Animals in Research: Reporting In Vivo Experiments) guidelines. In addition, MD is trained and licensed to conduct animal research by the European Laboratory Animal Science (FELASA) and national authorities (DGVA).

2.5.2. Sample preparation and biochemical analysis

Stored animals were individually homogenized in 4 mL of cold PBS at pH 7.7 ± 0.1 using a tissue homogenizer (Tissue Master 125, Omni, USA). Tissue homogenates were transferred to microtubes (1.5 mL) and then centrifuged at 15,0000 g, for 10 min at 4 °C, and supernatants stored at −80 °C. Thereafter, the Bradford protein assay was used to determine the total protein concentration of the previously prepared samples (Bradford, 1976), and all further results obtained in the biochemical assays were normalized to the total protein mass herein determined. Several biochemical biomarkers were thereafter exploited to evaluate the influence of THEDES and 5-FU exposure on the zebrafish model. These include enzymatic activity of catalase (CAT), glutathione-S-transferase (GST), superoxide dismutase (SOD), glutathione peroxidase (Gpx), acetylcholinesterase (AChE), and caspase-3, but also the impact on lipid peroxidation

(LPO) and total antioxidant capacity (TAC), as previously reported (Ferreira et al., 2022; Figueiredo et al., 2020; Lopes et al., 2018).

2.5.3. Statistical analysis

Statistical analysis of the resulting data was carried out using GraphPad Prism 9.0 (GraphPad Software, USA). All results are expressed as mean ± standard deviation (SD). Significant differences were calculated as a comparison between control and different compounds, and P-values smaller than 0.05 were considered statistically significant (confidence interval of 95 %). The statistical differences are represented by different numbers of "*". To assess significant statistical differences, first the normal distribution of results was tested using the Shapiro-Wilk test. When the results followed a normal distribution, One-Way ANOVA was used to perform the comparisons following Dunnett or Tukey multiple comparison test. When results did not follow a normal distribution, Kruskal-Wallis test was performed. To facilitate the comparison of the results obtained among the different biomarkers an integrated biomarker response index (IBR) was calculated as described elsewhere with all biomarkers compared using Z = Y (Beliaeff and Burgeot, 2002; Cruz et al., 2023).

3. Results and discussion

3.1. Permeability and cellular transport

Since CRC carcinogenesis highly relies on inflammation, its control is a key aspect of the desired therapeutic profile of an anti-CRC drug (Coussens and Werb, 2002; Apple et al., 2016). Non-steroidal anti-inflammatory drugs such as Ibu, not only have well-described anti-inflammatory activity, but also have preventive and anticancer activity, for example, through the inhibition of β-catenin nuclear activation in CRC cells (Greenspan et al., 2011; Zappavigna et al., 2020). Nevertheless, such anti-inflammatory drugs activity is often limited by its low bioavailability in physiological media, as a consequence of its poor solubility although having high permeability (class II on biopharmaceutics classification system) (Nascimento et al., 2021). In this context, eutecticity has been described in the optimization of such APIs bioavailability (Zainal-Abidin et al., 2019; Duarte et al., 2017; Santos and Duarte, 2021). Table 1 summarizes the systems prepared and studied in this work.

The effect of THEDES on Ibu's permeability and cellular transport was herein investigated. First, using a glass diffusion apparatus (Table 2), it is possible to recognize that Thy:Ibu (3:1) promotes a significant increase in Ibu permeability ($^*p \leq 0.05$), however when combined with POH this API does not experience a permeability increase (Fig. S1–A).

Furthermore, POH:Ibu (3:1) promotes a significant increase ($^*p \leq 0.05$) in Ibu's diffusion coefficient, while Thy:Ibu (3:1) and POH:Ibu (8:1) do not (Fig. S1–B). Since the diffusion coefficient is a parameter correlating API amount diffused within time (Duarte et al., 2017; Santos et al., 2019), from the obtained results it is possible to infer that the combination of POH with Ibu as a eutectic system in a 3 to 1 M ratio presents a faster diffusion of Ibu through the membrane. This result is highlighted in Fig. 1, where the profile of Ibu permeability can be observed over time.

These permeability and diffusion results highlight that, although all these THEDES combine Ibu with a terpene, there are differences not only when varying the terpene but also when altering their molar ratio. This was also emphasized in a previous work, where combining Me with Ibu promoted a much higher permeability increase, while when using Safranal (Saf) this tendency was not observed (Pereira et al., 2022).

In a second step, Ibu permeability and cellular transport were investigated using a colonic cell model, which allows a more representative *in vitro* microenvironment reconstitution (Santos and Duarte, 2021). The obtained results are presented in Table 3, where it is possible to observe that the eutectic formulations do not promote beneficial effects on Ibu permeability, with a significant decrease observed for Thy:Ibu (3:1) ($p \leq 0.0001$), POH:Ibu (3:1) ($p \leq 0.001$) and Me:Ibu (3:1) ($p \leq 0.0001$) (Fig. S2).

Interestingly, the permeability studies using this cell model revealed contrasting results in comparison with what was previously obtained using a synthetic membrane. These results are highlighted in Fig. S2–A, where the profile of Ibu permeability can be observed over time.

In Fig. 2, it is possible to recognize that these results are a consequence of Ibu intracellular accumulation, since the cellular uptake is significantly increased in all tested eutectic formulations, with a highlight for Thy:Ibu (3:1). Furthermore, the maintenance of TEER values (data not shown) reinforces the non-cytotoxicity of the tested concentrations towards normal colonic cells.

It has been described that Ibu is easily absorbed in the intestinal epithelium by passive transport (Omkvist et al., 2010). On the other hand, although terpenes such as Me, Thy and POH, transport is mainly passive, they may stimulate paracellular transport of large molecules by interacting with tight junctions (Edelblum and Turner, 2015; Heinlein et al., 2014). The observed results contrast with such reports since, in this case, combining a terpene with Ibu as a eutectic, did not stimulate paracellular but instead transcellular transport. Ultimately, in this context, THEDES seem to contribute to less transport from the apical to the basolateral side of the

Table 1
Summary of the THEDES, corresponding individual components and molar ratios used in this work.

Terpene	NSAID	Abbreviation	Molar ratio
Menthol (Me)	Ibuprofen (Ibu)	Me:Ibu	3:1
Thymol (Thy)		Thy:Ibu	3:1
Perillyl alcohol (POH)		POH:Ibu	3:1 and 8:1
Limonene (Lim)		Lim:Ibu	4:1 and 8:1

Table 2
Permeability results and diffusion coefficients obtained for Ibu in THEDES and in powder forms, using a synthetic PES-U membrane. Data indicated as mean ± SD. *p ≤ 0.05, as the statistical significance compared with the control.

	Permeability (10^5 cm s^{-1})	Diffusion coefficient (10^6 cm^2 s^{-1})
Thy:Ibu (3:1)	5.76 ± 1.31 (*)	2.52 ± 0.87
POH:Ibu (3:1)	4.45 ± 0.03	4.24 ± 0.93 (*)
POH:Ibu (8:1)	1.92 ± 0.58	3.13 ± 1.15
Me:Ibu (3:1)	14.00 ± 1.53[a]	4.32 ± 0.34[a]
Ibu	3.52 ± 0.26 [b]	1.30 ± 0.22 [b]

[a] retrieved from(Duarte et al., 2017).
[b] retrieved from(Pereira et al., 2022).

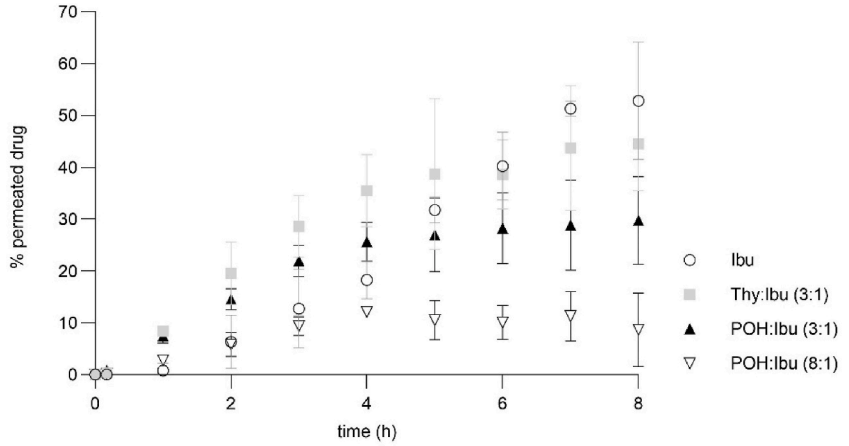

Fig. 1. Permeation profile obtained using a synthetic PES membrane in physiological-like conditions (PBS solution at 37 °C) of Ibu alone, Thy:Ibu (3:1), POH:Ibu (3:1) and POH:Ibu (8:1). Results were obtained from three independent experiments performed in triplicate and herein expressed in terms of percentage of permeability. Data indicated as mean ± SD.

Table 3
Estimate apparent permeability (Papp), Ibu concentration on apical and basolateral side of the transwell apparatus, and cellular uptake obtained for Ibu in THEDES and in powder. Data indicated as mean ± SD. *p ≤ 0.05, **p ≤ 0.01, ***p ≤ 0.001 and ****p ≤ 0.0001, as the statistical significance compared with the control for Papp.

	Papp (10^5 cm s^{-1})	Final concentration on apical side (mg mL^{-1})	Final concentration on basolateral side (mg mL^{-1})	Estimated cellular uptake (mg mL^{-1})
Thy:Ibu (3:1)	3.58 ± 1.1 (****)	0.091 ± 0.00	0.003 ± 0.00	0.093
POH:Ibu (3:1)	0.93 ± 0.1 (****)	0.008 ± 0.00	0.000 ± 0.00	0.031
POH:Ibu (8:1)	5.39 ± 0.2	0.134 ± 0.00	0.004 ± 0.00	0.056
Me:Ibu (3:1)	4.80 ± 0.1 (***)	0.059 ± 0.00	0.002 ± 0.00	0.034
Ibu	5.72 ± 2.7	0.364 ± 0.02	0.011 ± 0.00	0.125

transwell plate. Pereira and coworkers also described this cellular uptake tendency for THEDES combining Lim with Ibu in 4:1 and 8:1 M ratios, respectively (Pereira et al., 2019).

Finally, it can be hypothesized that an improvement in the bioavailability of this API may lead to a reduction of its effective dose - the minimum amount of a therapeutic agent required to produce the desired therapeutic effect - which not only mitigates potential side effects but also positively impacts sustainability metrics by lowering the amount of drug needed and consequently reducing the overall production and associated waste.

3.2. THEDES bioactivity

3.2.1. Intracellular ROS

ROS play an important role in modulating inflammatory pathways, and when enhanced in tumor microenvironment, and specifically in human colonic mucosa, ROS contribute to the epithelial-mesenchymal transition, which leads to increased proliferation,

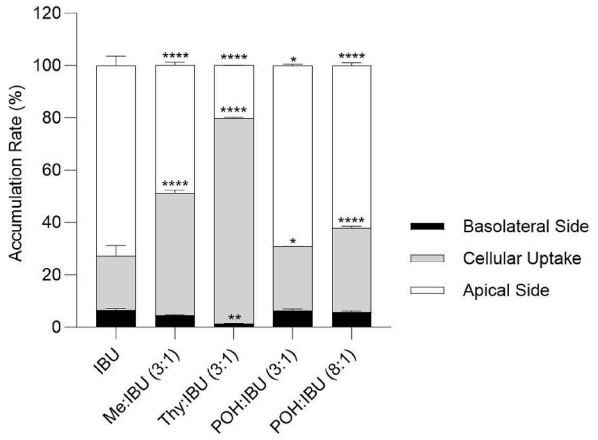

Fig. 2. Accumulation rate and cell transport using a differentiated Caco-2 transwell cell model for Ibu, Me:Ibu (3:1), Thy:Ibu (3:1), POH:Ibu (3:1) and POH:Ibu (8:1). Results were obtained from three independent experiments performed in triplicate and herein expressed in terms of percentage of accumulation rate at the apical and basolateral sides of the transwell plate, and cellular uptake. Data indicated as mean ± SD. *p ≤ 0.05, **p ≤ 0.01, ***p ≤ 0.001 and ****p ≤ 0.0001, as the statistical significance compared with the control.

invasion and migration (Hanahan, 2022; Lin et al., 2018; Huang et al., 2019). Thus, controlling ROS presence in CRC cells represents a complementary strategy to cope with cancer development and progression.

In this work, an HT29 cell model was chosen since these CRC cells have high levels of basal stress, hence presenting high levels of ROS production (Huang et al., 2019). Regarding the results obtained for the POH-based systems (Fig. 3 - B), POH:Ibu (3:1) and POH: IBU (8:1) do not seem to influence ROS production at the tested concentrations, nor their corresponding individual components. Even though, in previous reports, its terpene precursor, Lim, in combination with Ibu revealed protective action towards oxidative stress (Pereira et al., 2019).

In contrast, Thy:Ibu (3:1) (Fig. 3 - A) seems to promote a significant decrease ($p \leq 0.001$), more than two-fold, of oxidative species. Such oxidative stress reduction may ultimately downregulate CRC carcinogenesis by reducing genomic instability occurring via oxidative DNA damage but also downregulate ROS-induced inflammatory cascade. When looking to its corresponding individual components, it is possible to observe the inverse tendency since they seem to increase ROS. This highlights the difference between the individual compounds acting alone, in comparison with the synergetic effect observed as a THEDES. This result may be an outcome of the cellular uptake tendency previously described (Section 3.1) for the Thy-based system in the cellular transport studies.

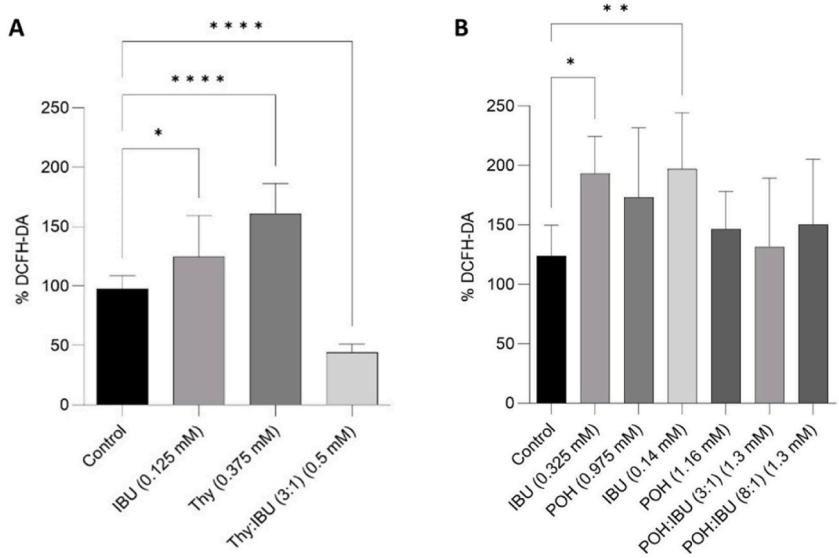

Fig. 3. Intracellular ROS results obtained for (A) Thy:Ibu (3:1) and respective individual compounds, with Thy and Ibu at the same concentration present in THEDES, (B) POH:Ibu (3:1) and POH:Ibu (8:1), and their respective corresponding individual compounds at the same concentration present in THEDES. Results were obtained from three independent experiments performed in triplicate. Data indicated as mean ± SD. *p ≤ 0.05, **p ≤ 0.01, ***p ≤ 0.001 and ****p ≤ 0.0001, as the statistical significance compared with the control.

In a previous report, terpenes, such as Me and Saf, combined with Ibu revealed the Me:Ibu (3:1) system acting as a protective agent for oxidative stress in HT29, while Saf:Ibu (3:1) and Saf:Ibu (4:1) did not (Pereira et al., 2022). Moreover, it has been reported that low levels of ROS lead to downregulation of the inflammatory cascade, but it is also known that excessive high levels of ROS promote cancer cell death (Lin et al., 2018).

Hence, considering the obtained results, we hypothesize that the herein discussed THEDES do not induce cancer cell death via ROS increase, so its reported antiproliferative effect must have a different cause. Nevertheless, these THEDES may play an interesting role as protective agents towards oxidative stress and ultimately inflammation in CRC.

3.2.2. LDH release

There are several reports hypothesizing that DES-induced cancer cell death occurs via cell membrane disruption, following a necrotic form of cell death (Zainal-Abidin et al., 2019; Hayyan et al., 2015). In Fig. 4, it is possible to observe that all tested THEDES induce cancer cell death via membrane disruption, but only at concentrations three times higher than their corresponding reported half maximal effective concentration (EC_{50}). Hence, these results suggest that membrane disruption has not been the primary cause of HT29 cell death after exposure to Thy:Ibu (3:1), POH:Ibu (3:1), POH:Ibu (8:1), Lim:Ibu (4:1) and Lim:Ibu (8:1).

In a previous report, Pereira and coworkers described that Me:Ibu (3:1) promotes cell membrane disruption at its EC_{50}, so within its reported therapeutic window, while Saf:Ibu (3:1) and Saf:Ibu (4:1) only induce disruption at higher concentrations than its EC_{50}

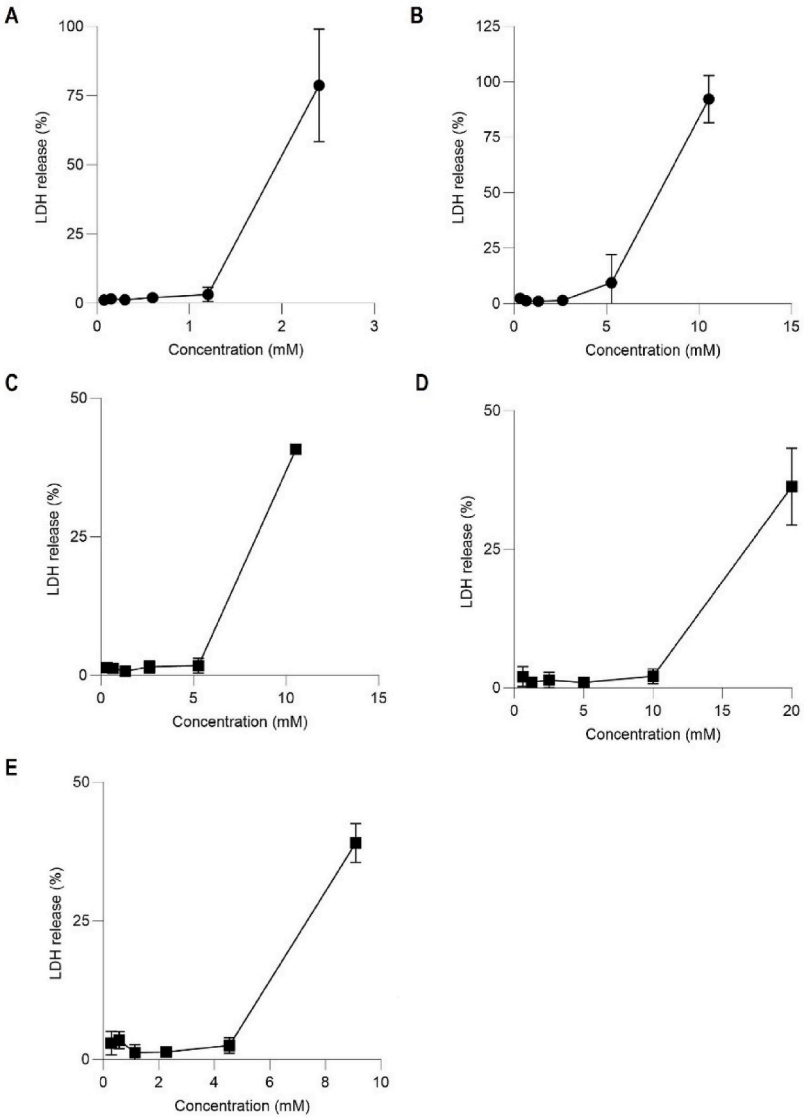

Fig. 4. LDH released by HT29 cells after exposure to (**A**) Thy:Ibu (3:1), (**B**) POH:Ibu (3:1), (**C**) POH:Ibu (8:1), (**D**) Lim:Ibu (4:1), and (**E**) Lim:Ibu (8:1), at different concentrations. Results were obtained from three independent experiments performed in triplicate. Data indicated as mean ± SD.

(Pereira et al., 2022). This disruption may be related with the hydrophobic nature of the herein used terpenes that allows them to interact with the phospholipid cell membrane bilayer, but may prevent their full cellular uptake. Thus, the observed cancer cell death upon THEDES exposure could be related to alterations in cell membrane mechanical fluidity. This, in turn, compromises its stability, which is essential, especially in cancer cells that have increased abnormal cell division rates. This alteration can be of most importance since the mechanical disturbance may cause membrane disruption and eventual cell death (Duelund et al., 2012; Oliveira and Duarte, 2021).

Thus, the herein obtained results suggest that the tested THEDES induce HT29 death via a different route and highlight that, although all these THEDES are based on the combination of a terpene with Ibu, different combinations and even different molar ratios promote a different impact in CRC cells.

3.2.3. *Apoptosis via caspase-3/7*

For a better understanding of how these THEDES could be exerting the reported antiproliferative action towards HT29, the induction of programmed cell death via the caspase-3/7 pathway was evaluated. In Fig. 5, it is possible to observe that all tested THEDES promoted cell death by inducing apoptosis, when compared with the control of non-exposed cells. Interestingly, although there have been reports on different terpenes and anti-inflammatory drugs as inducers of apoptosis (Elsisi et al., 2005; Farrugia and Balzan, 2013; Yang and Dou, 2010), in Fig. 5 it is observable that the compounds alone have minor or no effect. Hence, this programmed cell death

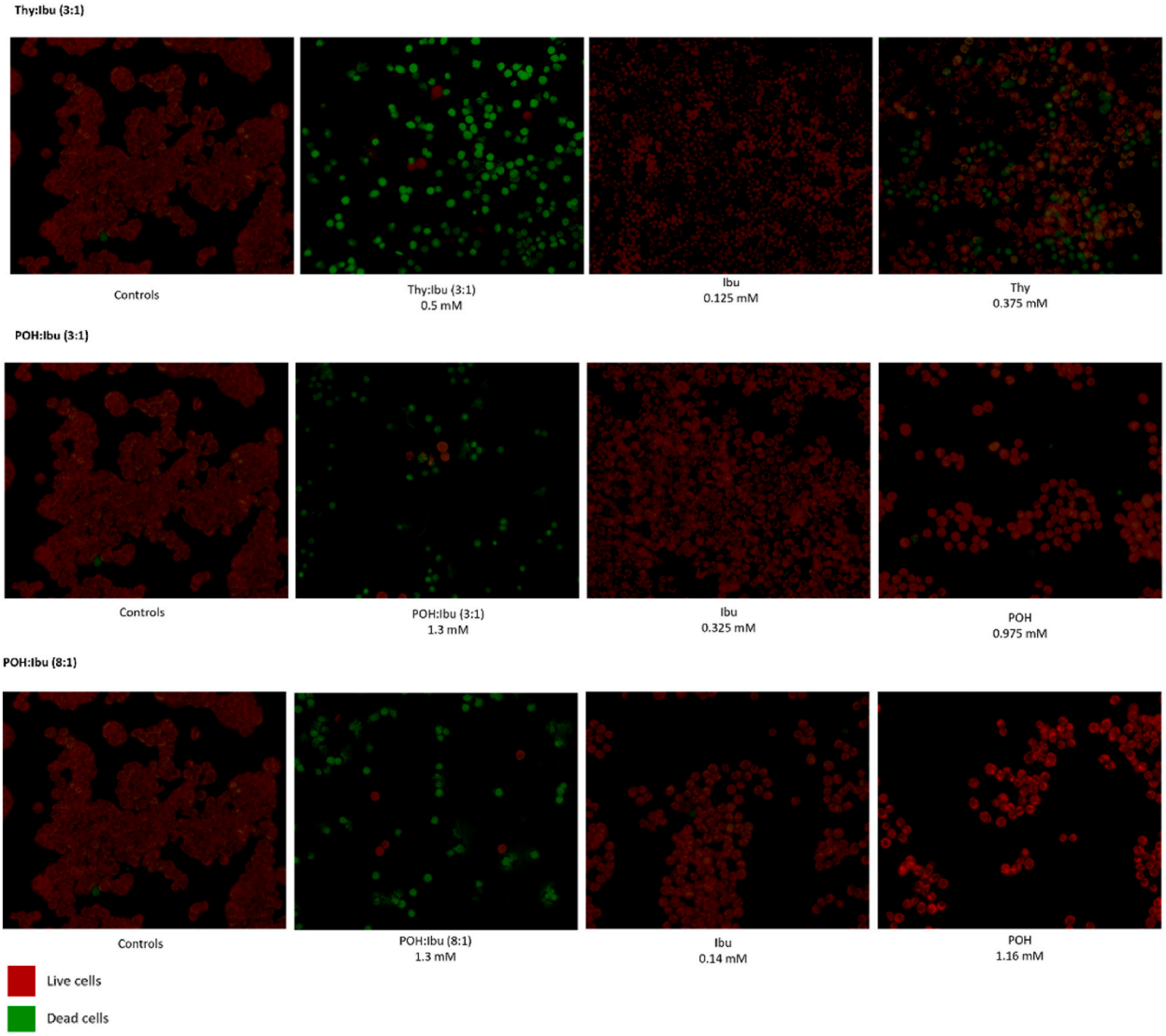

Fig. 5. Micrographs of apoptosis induction via caspase-3/7 pathway for Thy:Ibu (3:1), POH:Ibu (3:1) and POH:Ibu (8:1), and their corresponding individual compounds using the same concentrations as if they were in the eutectic formulation, in comparison with negative control of non-exposed CRC cells.

induction is enhanced when the compounds are presented to the cancer cells as a eutectic formulation.

These results follow what was previously reported for Me:Ibu (3:1), Saf:Ibu (3:1) and Saf:Ibu (4:1) (Pereira et al., 2022), suggesting that the main action of these THEDES to prevent CRC cell proliferation is, in fact, through the induction of apoptosis via the caspase-3/7 pathway. On the other hand, it is interesting to mention that Lim:Ibu (4:1) and Lim:Ibu (8:1) do not promote apoptosis via this pathway (Pereira et al., 2019). This once more emphasizes the heterogenic bioactive profile of THEDES towards CRC cells and the tailor-made therapeutic possibilities it unlocks.

3.3. Metabolomic landscape of CRC cells upon THEDES exposure

3.3.1. THEDES influence on HT29 cells endometabolome

The influence of THEDES on CRC cells endometabolome was herein investigated by a GC-MS-based metabolomics approach. The GC-MS metabolomic analysis identified 16 metabolites in the intracellular environment, from which some suffer variations as a consequence of THEDES exposure (Table S1).

To investigate this, first the analytical reproducibility of the GC-MS experimental data was confirmed by an unsupervised statistical analysis (PCA). For this, all samples and quality controls (QC) were included, and the statistical analysis revealed well-defined QCs clusters (Fig. S3–A).

Further, the unsupervised PCA and supervised multivariate analyses (PLS-DA) were performed considering the comparison between the intracellular metabolome of non-exposed cells (control) and cells exposed to the different THEDES. As expected based on the previously described results, different outcomes were observed here depending on the combination of compounds and their molar ratios in the THEDES. The results for Me:Ibu (3:1) and Lim:Ibu (4:1) revealed a good separation between the control and the exposed cells, and POH:Ibu (8:1) also revealed a separation in the PLS-DA model although less robust ($Q^2 = 0.35$). The cells exposed to Thy:Ibu (3:1), Lim:Ibu (8:1) and POH:Ibu (3:1), did not reveal any separation between the control and exposed cells.

Furthermore, a variable importance to the projection (VIP) score was performed (Fig. 6) to assess which could be the metabolites responsible for the difference previously observed between the control and cells exposed to THEDES. Several metabolites such as lactate, oxalate, *myo*-inositol, 5-oxoproline, glycine, 1-octadecanol, glucose and palmitic acid revealed high importance (VIP >1) to discriminate between THEDES exposed cells and the control.

When comparing control cells with THEDES-exposed cells, amongst the 16 metabolites detected in the GC-MS analysis of the endometabolome, statistical significance was only found for i) lactate, in cells exposed to Me:Ibu (3:1) and Lim:Ibu (4:1) (Fig. 7), ii) myo-inositol, in cells exposed to Me:Ibu (3:1), POH:Ibu (8:1) and Lim:Ibu (4:1) (Fig. 7), iii) 1-octadecanol, in cells exposed to Lim:Ibu (4:1) (Fig. 7), iv) and palmitic acid, in cells exposed to POH:Ibu (8:1) (Fig. 7).

The effect size of each metabolite significantly altered is summarized in Table 4 with the potentially affected metabolic pathways.

From these results it is possible to observe a heterogeneous outcome on HT29 cancer cells endometabolome upon exposure to THEDES. HT29 exposed to Me:Ibu (3:1), POH:Ibu (8:1) and Lim:Ibu (4:1), promoted a deleterious effect in the levels of *myo*-inositol, with highlight for the Me-based system. This metabolite is involved in several key metabolic pathways for cell homeostasis and proliferation, mostly related to cell signaling and nucleotide synthesis (Bridges and Saltiel, 2012). It works as a building block of a cellular language via i) insulin signaling, ii) PI3K/Akt signaling, iii) endocytosis, iv) vesicle trafficking, v) cell migration, vi) proliferation and vii) apoptosis (Gillaspy, 2011). But also plays a pivotal role in nucleotide synthesis in the incorporation of adenine and guanosine (Tsukagoshi et al., 1966). Thus, deregulation of this pathway may disrupt homeostasis and promote carcinogenesis (Tan et al., 2015). Hence, THEDES-induced *myo*-inositol depletion seems to compromise such metabolic pathway, downregulating it, which ultimately contributes to the induced cell death by apoptosis described in the previous section.

Furthermore, HT29 exposure to POH:Ibu (8:1) and Lim:Ibu (4:1) seem to interfere with lipid metabolism, upregulating it, resulting in a significant increase ($p \leq 0.05$) of palmitic acid and 1-octadecanol, respectively, when compared to the control. Both catabolic and anabolic pathways of lipid metabolism play an important role in cell activity related to i) membrane structure and function, ii) intracellular signaling pathways, iii) transcription factor activity and consequent gene expression, iv) and production of bioactive lipid mediators (Calder, 2015). Considering cancer biology, fatty acids such as palmitic acid are mostly recognized as substrates for energy production in these highly proliferating cells (Cucchi et al., 2020). Thus, the observed increase in palmitic acid could be associated with the reported Warburg effect, where cancer cells prefer the anaerobic glycolysis pathway for energy production. To cope with the energy demand of fast proliferating cells, cancer cells may rely on fatty acids for energy production via β-oxidation (Cucchi et al., 2020). Nevertheless, saturated and unsaturated fatty acids crucial role in cancer cells sensing has also been reported since they differentially regulate the transcriptional activity of the retinoic acid receptor (RAR) and peroxisome proliferator-activated receptors (PPARβ/δ). Meaning that saturated fatty acids, such as palmitic acid, by activating RAR and inhibiting PPARβ/δ, are capable of suppressing cancer cell proliferation (Levi et al., 2015). Since in the previously obtained results it was observed that POH:Ibu (8:1), in this concentration, promotes cell death, we hypothesize that this could be the case of fatty acid synthesis working as suppressors of cancer cell proliferation instead of contributing for energy production.

Moreover, the upregulation detected for the fatty alcohol 1-octadecanol suggests an altered fatty alcohol metabolism in the studied cells (Lam et al., 2023). This accumulation can be associated with a deficient activity of fatty aldehyde dehydrogenase (FALDH), which is an enzymatic component of fatty alcohol:NAD oxidoreductase (FAO) necessary for fatty alcohol metabolism (Rizzo et al., 2008). Furthermore, 1-octadecanol participates in the plasmalogen synthesis (Jewison et al., 2014). Specifically for CRC, alterations in plasmalogen synthesis and its subclasses have been associated with phospholipases C and D activity reduction and increased activity of phosphocholine cytidyltransferase. Such alterations result in generally elevated phospholipid and the phosphatidylethanolamine plasmalogen specie content (Dueck et al., 1996; Gerbig et al., 2012). Since plasmalogens highly contribute to cell membrane fluidity

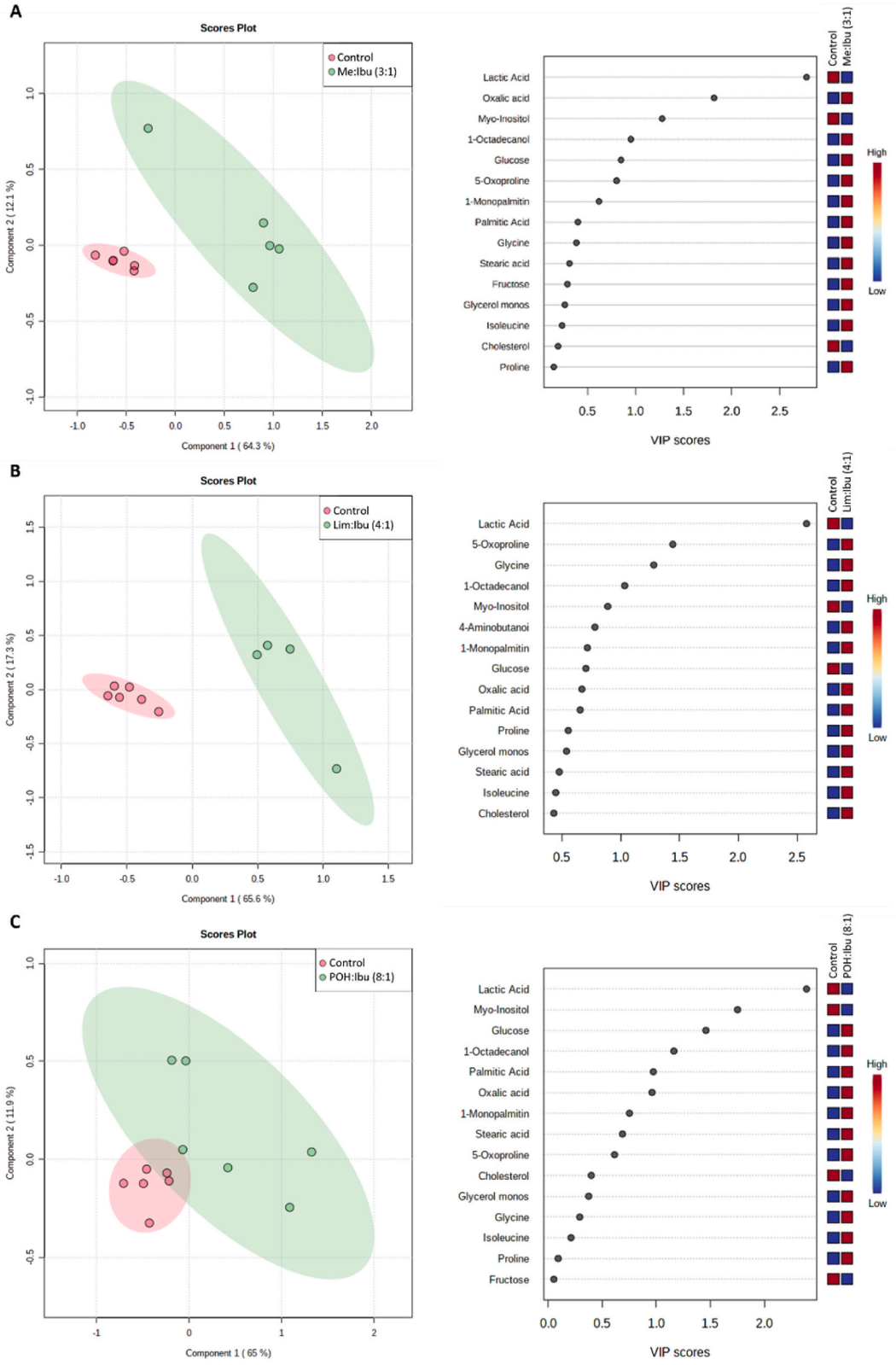

(caption on next page)

Fig. 6. Impact of THEDES on the endometabolome landscape of HT29 cells. (A) PLS-DA scores scatter plot (left) obtained for negative control of non-exposed cells (red circles, n = 8) vs. cells exposed to Me:Ibu (3:1) (green circles, n = 8) and corresponding VIP score plot (right). (B) PLS-DA scores scatter plot (left) obtained for negative control of non-exposed cells (red circles, n = 8) vs. cells exposed to Lim:Ibu (4:1) (green circles, n = 8) and corresponding VIP score plot (right). (C) PLS-DA scores scatter plot (left) obtained for negative control of non-exposed cells (red circles, n = 8) vs. cells exposed to POH:Ibu (8:1) (green circles, n = 8) and corresponding VIP score plot (right).

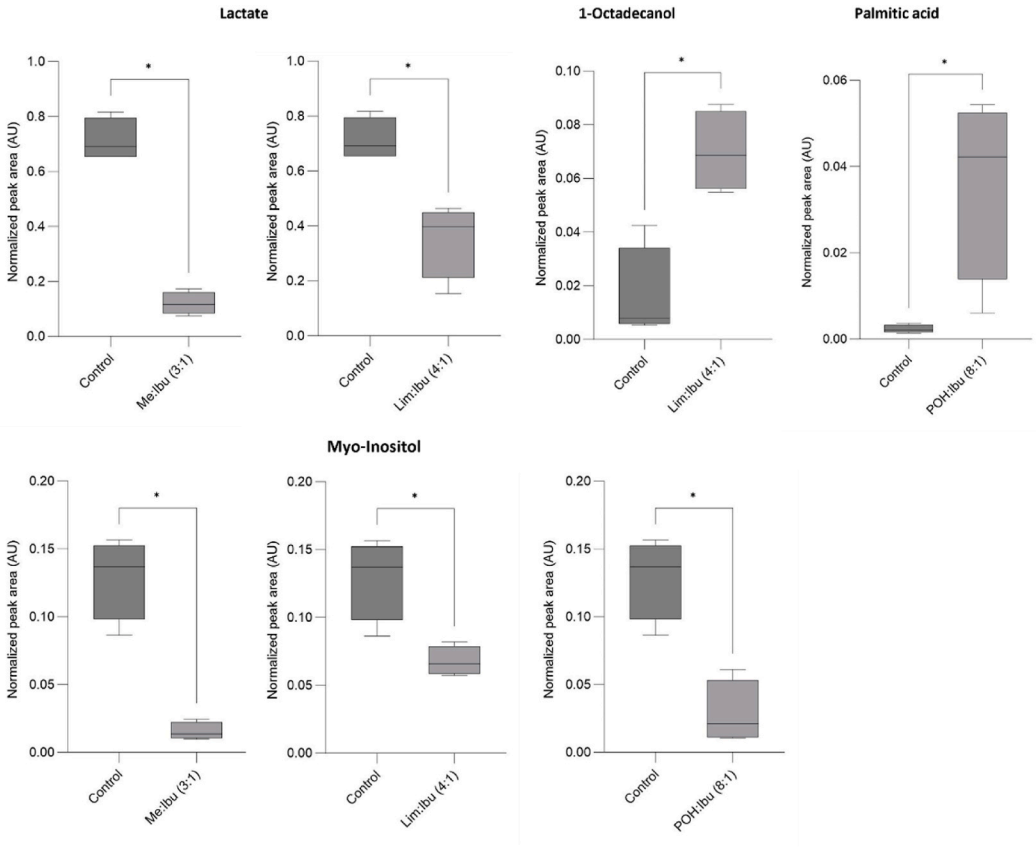

Fig. 7. Boxplot representation of the intracellular metabolites significantly influenced upon exposure to Me:Ibu (3:1), Lim:Ibu (4:1) and POH:Ibu (8:1). Data indicated as median and minimum and maximum. *p ≤ 0.05, **p ≤ 0.01, ***p ≤ 0.001 and ****p ≤ 0.0001, as the statistical significance compared with the control.

and ultimately its stability, we hypothesize that the observed upregulation by POH:Ibu (8:1) of 1-octadecanol could contribute to an excessive plasmalogen synthesis that, in the end, results in membrane instability and the cell death induction previously observed.

In contrast, from the depletion observed in lactate in HT29 cells exposed to Me:Ibu (3:1) and Lim:Ibu (4:1), these THEDES seem to have a deleterious effect on the anaerobic glycolysis pathway as lactate is its resulting metabolite. Since these cells can be considered to be in anaerobic-like conditions while experiencing the Warburg effect (DeBerardinis and Chandel, 2020), these THEDES seem to compromise cancer cell main choice for energy production and in this way compromise their viability.

3.3.2. THEDES influence in HT29 cells exometabolome

Following the description of THEDES influence on HT29 cells endometabolome, it was investigated by GC-MS-based metabolomics what might be happening on cell's exometabolome. The GC-MS metabolomic analysis identified 17 metabolites (aldehydes and ketones) in the extracellular environment, in which some suffer variations as a consequence of THEDES exposure (Table S2).

Once more, different results for the different combinations of compounds and molar ratios composing THEDES were obtained. The results for Thy:Ibu (3:1) revealed a good separation between the control and exposed cells; POH:Ibu (3:1) and POH:Ibu (8:1) also revealed a separation in the PLS-DA models. In contrast, HT29 cells exposed to Me:Ibu (3:1), Lim:Ibu (4:1) and Lim:Ibu (8:1), did not reveal any separation between the control and exposed cells in both PCA and PLS-DA models (Fig. 8).

To better understand which could be the metabolites promoting such separation, a VIP score projection was performed. In Fig. 8 it is possible to observe from VIP score 1 upward several metabolites, such as methylglyoxal, 4-methyl-2-pentanone, cyclohexanone, acetaldehyde and acetone.

Among the 17 metabolites detected in the GC-MS analysis of the extracellular environment, statistical significance was only found

Table 4
Altered metabolites and potentially affected metabolic pathways resultant from the endometabolome analysis of THEDES exposed cells compared with control cells.

Metabolite	Alterations caused by each THEDES vs control			Metabolic pathways
	Me:Ibu (3:1)	POH:Ibu (8:1)	Lim:Ibu (4:1)	
Lactate	−2.35 ± 1.60 (*)	–	−3.69 ± 1.98 (*)	Glycolysis/Gluconeogenesis; Pyruvate metabolism
Myo-inositol	−3.76 ± 1.91 (*)	−2.98 ± 1.58 (*)	−2.08 ± 1.46 (*)	Galactose metabolism; Inositol phosphate metabolism; Biosynthesis of nucleotide sugars; Phosphatidylinositol signaling system
1-Octadecanol	–	–	3.89 ± 2.05 (*)	Plasmalogen Synthesis
Palmitic acid	–	2.21 ± 1.37 (*)	–	Fatty acid metabolism

for methylglyoxal, when comparing cells exposed to Thy:Ibu (3:1), POH:Ibu (3:1), and POH:Ibu (8:1) with the control (Fig. 9); and for acetaldehyde for the POH:Ibu (8:1) exposed cells compared with the control (Fig. 9).

The effect size of each metabolite significantly altered is summarized in Table 5 with the potentially affected metabolic pathways.

From these results it is possible to observe that HT29 exposed to these THEDES produces an augmentation of methylglyoxal in the extracellular environment and a lower acetaldehyde consumption from the external media, in comparison with the control.

It has been reported that the Warburg effect is one of cancer cells key metabolic alterations. Such alteration reflects cells preference for the anaerobic glycolysis energy production pathway (DeBerardinis and Chandel, 2020). This results in an increased production of glycolysis intermediates where, among them, there is methylglyoxal as a glucose-derived highly reactive dicarbonyl (Thornalley et al., 1999). Although this aldehyde is well-known to participate in glycine, serine and threonine metabolism (Kanehisa et al., 2023), regarding cancer cells, it has been hypothesized that methylglyoxal major role can be hormetic, working both as pro-tumorigenic and as an anti-cancer (Leone et al., 2021). The intracellular presence of this metabolite is mainly controlled by the glyoxalase system, where at low concentration, methylglyoxal results in beneficial effects allowing cancer cells to avoid apoptosis and enhance cell proliferation, but when the threshold of dicarbonyl stress is exceeded the effect is the opposite and cell death is inevitable, due to DNA and protein synthesis inhibition, and cellular respiration (Reiffen and Schneider, 1984).

In Fig. 9, it is possible to observe that the control cells consumed methylglyoxal reducing its levels in comparison with the blank. In contrast, the presence of high levels of methylglyoxal in extracellular medium of cells exposed to POH:Ibu (8:1), in comparison with the control, suggests that this THEDES upregulates such metabolite production or impairs cell's inherent glyoxalase system, which ultimately may lead to cell death, as observed in the previous sections. Although Thy:Ibu (3:1) and POH:Ibu (3:1) also induce apoptosis (Fig. 5), herein it was observed that these THEDES did not induce methylglyoxal production nor allowed its significant consumption by the cells. This could be related to the lower terpene presence in the eutectic system formulation.

Furthermore, acetaldehyde participates in different key metabolic pathways such as glycolysis and pyruvate metabolism (Kanehisa et al., 2023). However, increased levels of acetaldehyde promote several deleterious effects in cells by forming protein, DNA, and phospholipid adducts that result in DNA lesions (Rodriguez and Coveñas, 2021). Hence, when looking to the results obtained for POH:Ibu (8:1), particularly concerning the presence of acetaldehyde in the extracellular environment, in comparison to the blank, it is possible to conclude that there was a consumption from the external media by the control cells, which can be related to the acetaldehyde uptake for pyruvate metabolism for energy production (Guittin et al., 2023). Nonetheless, cells exposed to this eutectic system seem to experience an impairment in acetaldehyde metabolism, since its presence remains similar to the blank. This fact could mean that its intracellular accumulation and an impairment of aldehyde dehydrogenases may result in cell death by acetaldehyde-forming adducts (Rodriguez and Coveñas, 2021).

3.4. *THEDES effect in zebrafish*

To push forward the establishment of the herein described THEDES as anticancer therapeutic agents, a perception of their effect on more complex models as a whole organism is mandatory. For that, a preliminary systemic toxicity assessment, based on THEDES influence on multiple biomarkers (catalase (CAT), glutathione-S-transferase (GST), superoxide dismutase (SOD), glutathione peroxidase (Gpx), acetylcholinesterase (AChE), caspase-3, lipid peroxidation (LPO) and total antioxidant capacity (TAC)), was analyzed.

Since a multibiomarker approach was used, the integrated biomarker response (IBR) index was applied to evaluate the consequence of THEDES and 5-FU (positive control) exposure on such biomarkers (Devin et al., 2014).

Lim:Ibu (4:1) was the only tested condition promoting a different IBR response with a 37.79 index value, whereas the rest of the tested conditions presented a similar IBR index of 27.10 (Table 6).

In Fig. 10, it is possible to observe that Lim:Ibu (4:1) isolated position seems to be related to a higher CAT activity.

Besides IBR, a multiple comparison statistical test was also performed considering each individual biomarker. A significant increase ($p \leq 0.001$) of CAT and GST activities was observed after 5-FU exposure, in comparison with the control (Figure S4 – A and B). CAT and GST are associated with xenobiotic detoxification, by mediating oxidative stress responses (Tsuchida, 2002; Kehrer et al., 2010). Thus, from the results obtained for these two biomarkers it is possible to hypothesize that 5-FU is inducing oxidative stress in the exposed animals. This was somewhat expected since, although 5-FU is a standard drug for CRC treatment, it presents a wide range of negative side effects such as oxidative stress induction (Rtibi et al., 2021).

Contrasting results were observed for LPO since malondialdehyde (MDA) showed a significant decrease ($p \leq 0.05$) after 5-FU exposure (Fig. S3–C), suggesting a decrease of oxidative stress regarding this biomarker. It was also observed a GST increase in animals exposed to Lim:Ibu (4:1) and POH:Ibu (3:1), although less significative ($p \leq 0.05$) in comparison with 5-FU (Fig. S3–B).

Similarly to CAT, GPx is also an oxidoreductase, but ubiquitous in cytoplasm and mitochondria, which catalyzes the reduction of H_2O_2 to water and oxygen, and also the reduction of peroxide radicals to alcohols and oxygen (Pei et al., 2023). In animals exposed to Lim:Ibu (8:1), Thy:Ibu (3:1) and POH:Ibu (3:1) it was observed a GPx significative increase ($p \leq 0.05$ and $p \leq 0.01$) (Fig. S3–F), suggesting a response to fight the increased oxidative stress.

Further, AChE is the main cholinesterase enzyme and is responsible for breaking down acetylcholine (Ach) neurotransmitter in synapses, which terminates signal transmission, making it a biomarker for toxicity on the nervous system (Tsuchida, 2002).

From the obtained results, it is possible to recognize a significant increase ($p \leq 0.05$) for Thy:Ibu (3:1) and ($p \leq 0.001$) POH:Ibu (3:1) on the AChE activity (Fig. S3–G). An AChE imbalance has severe effects depending on whether there is an excess or deficiency of this enzyme. AChE inhibition can lead to an Ach accumulation, which can cause overstimulation of the nervous system, while its excess can lead to the rapid degradation of Ach and reduced signaling at cholinergic synapses (Tsuchida, 2002). AChE activity is often reduced by exposure to xenobiotics such as pesticides, but also in certain medical conditions such as dementia (Mladenović et al., 2018;

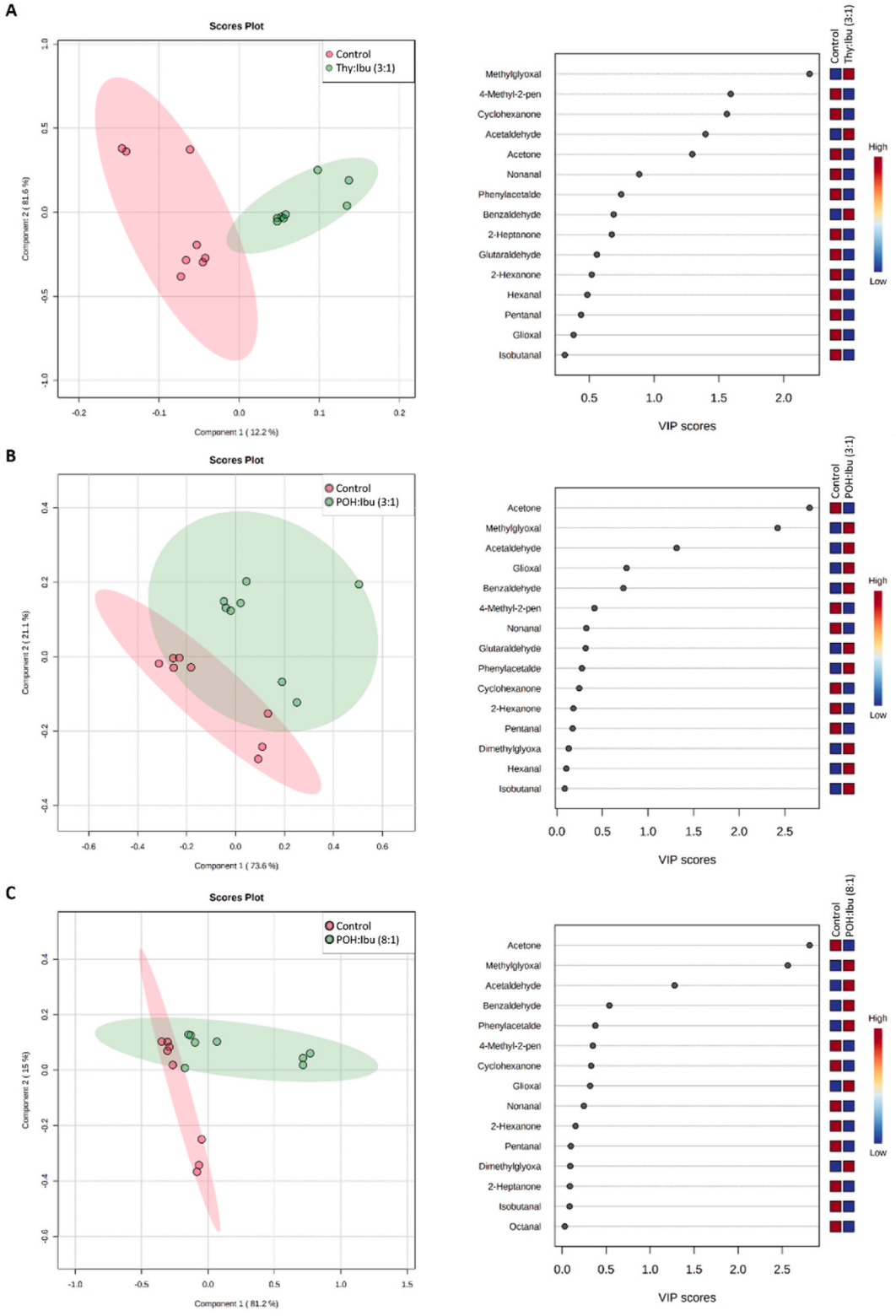

(caption on next page)

Fig. 8. Impact of THEDES on the exometabolome landscape of HT29 cells. (A) PLS-DA scores scatter plot (left) obtained for negative control of non-exposed cells (red circles, n = 8) vs. cells exposed to Thy:Ibu (3:1) (green circles, n = 8) and corresponding VIP score plot (right). (B) PLS-DA scores scatter plot (left) obtained for negative control of non-exposed cells (red circles, n = 8) vs. cells exposed to POH:Ibu (3:1) (green circles, n = 8) and corresponding VIP score plot (right). (C) PLS-DA scores scatter plot (left) obtained for negative control of non-exposed cells (red circles, n = 8) vs. cells exposed to POH:Ibu (8:1) (green circles, n = 8) and corresponding VIP score plot (right).

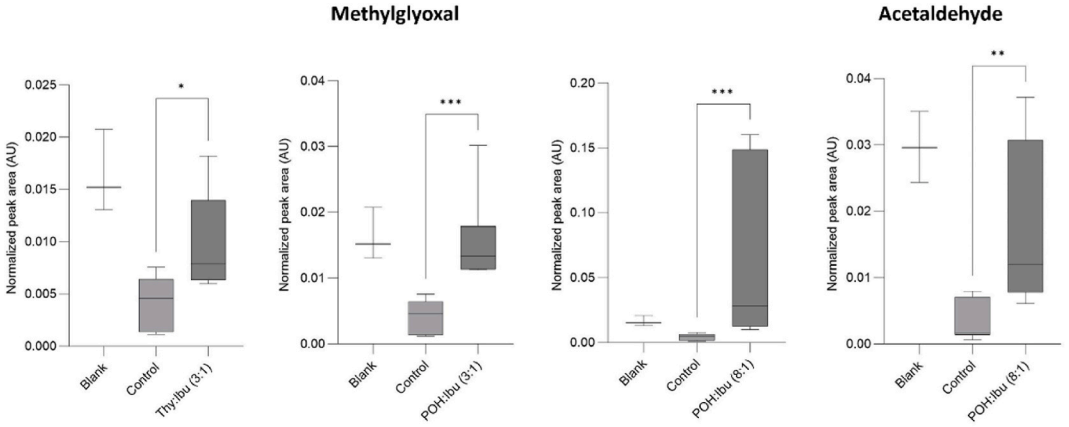

Fig. 9. Boxplot representation of the extracellular metabolites significantly influenced upon exposure to Thy:Ibu (3:1), POH:Ibu (3:1) and POH:Ibu (8:1). Data indicated as median and minimum and maximum. *p ≤ 0.05, **p ≤ 0.01, ***p ≤ 0.001 and ****p ≤ 0.0001, as the statistical significance compared with the control.

Table 5
Altered metabolites and potentially affected metabolic pathways resultant from the exometabolome analysis of THEDES-exposed cells compared with control cells.

Metabolite	Alterations caused by each THEDES vs control			Metabolic pathways
	Thy:Ibu (3:1)	POH:Ibu (3:1)	POH:Ibu (8:1)	
Methylglyoxal	1.55 ± 1.07 (*)	2.38 ± 1.24 (*)	1.33 ± 1.03 (*)	Glycine, serine and threonine metabolism; Pyruvate metabolism; Propanoate metabolism
Acetaldehyde	–	–	1.58 ± 1.08 (*)	Glycolysis/Gluconeogenesis; D-Amino acid metabolism; Glycerophospholipid metabolism; Pyruvate metabolism

Table 6
IBR index values obtained for each biochemical biomarker after THEDES and 5-FU exposure, and negative control.

Sample	Concentration (EC_{50}, mM)	IBR index value
Negative control	–	27.10
5-FU	25.98 [a]	27.10
Me:Ibu (3:1)	4.30	27.10
Thy:Ibu (3:1)	0.30	27.10
POH:Ibu (3:1)	1.32	27.10
POH:Ibu (8:1)	1.37	27.10
Lim:Ibu (4:1)	2.39	32.79
Lim:Ibu (8:1)	1.14	27.10

[a] retrieved from(Leong et al., 2016).

McGleenon et al., 1999). Nevertheless, it has been reported that in Alzheimer's disease, prevention of AChE inhibition could happen via oxidative stress-mediated compounds (Melo et al., 2003). So further studies on how these THEDES could beneficially influence such conditions could be of great interest.

Finally, although the individual multiple comparison statistical tests revealed significant differences between the control and animals exposed to 5-FU and THEDES for certain biomarkers, it is important to highlight that in such experiments external elements, such as gender, age and genetic predispositions, may also contribute to the obtained results, therefore it is reinforced the need for a data correlation analysis that better encompasses such diversity. In this way, Spearman's rank correlation coefficient was determined. The result did not reveal any significant correlation between the tested biomarkers upon exposure to the different systems (Fig. S3–I),

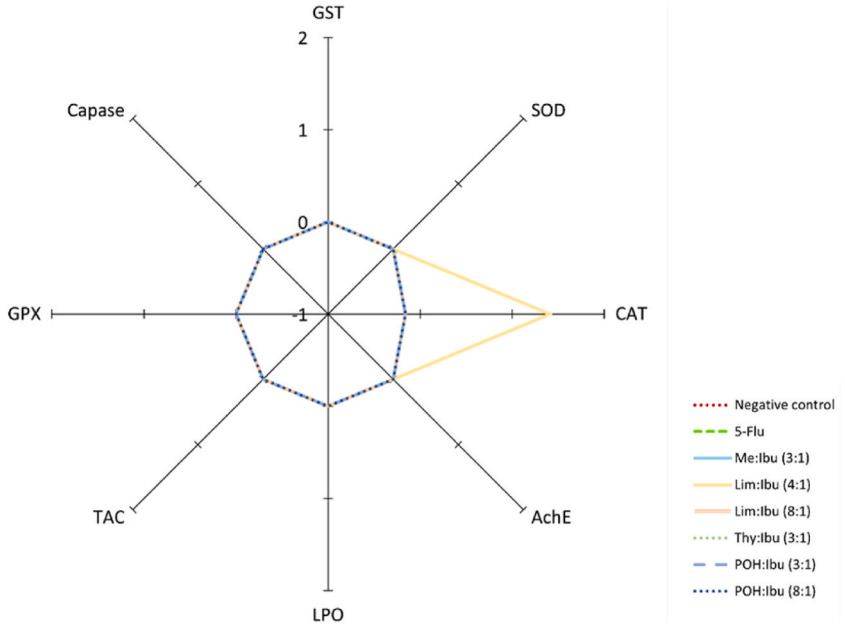

Fig. 10. IBR index values for each biochemical biomarker, after THEDES and 5-FU exposure, and negative control.

which could be corroborated by the previously reported IBR indexes, as a consequence of non-relevant systemic toxicity of these THEDES within the tested concentration range. Moreover, although in this assessment it was not observed a difference between THEDES and 5-FU, considering the ongoing pursue for greener and sustainable production processes in the pharmaceutical industry, since the starting molecules of these eutectics predominantly belong to the category of fine chemicals — which have a reported E-factor ranging between 5 and 50 kg of waste per kg of product (Lam et al., 2019; Sheldon, 2017). — it can be hypothesized that promoting large-scale applications of eutectics over traditional cancer APIs, as 5-FU, could potentially lead to a virtual 50 % reduction in the pharmaceutical industry's E-factor.

4. Conclusion

Complementing the knowledge on the reported selective anticancer action of THEDES combining Me, Thy, POH and Lim with Ibu, it was observed that combining these terpenes with Ibu as a eutectic formulation promotes Ibu cellular uptake, control of ROS production, and induce cancer cell dead via apoptosis. Moreover, THEDES exposure promoted alterations on the metabolite landscape of CRC cells, suggesting deleterious effects on essential metabolic pathways, such as lipid and anaerobic glycolysis energy production pathways, needed for cancer cell survival. Moreover, from a preliminary systemic toxicity evaluation these THEDES revealed non-relevant toxicity within the concentration range tested.

Furthermore, given the chemical nature of these eutectics, the first green chemistry principle that could be considered is "safer solvents and auxiliaries", but they also fall in other categories and, in particular, when considering the greenness of eutectics from the perspective of their use in pharmaceutical industry, where it is possible to encompass them in the following principles: i) atom economy, ii) less hazardous chemical synthesis, iii) design safer chemicals, iv) use of renewable feedstocks, v) design for degradation. Hence, although these industries are far from being green and, in a realistic perspective, it is still unlikely to aim for completely green production processes, the herein described premises for eutectic systems highlight them among the different sustainable solutions for developing effective therapeutic agents.

Finally, through the herein described results, the THEDES tailor-made characteristic is highlighted, since the system's bioactivity and potential anticancer activity vary depending on the combination of compounds and molar ratios. This opens up new ventures on the possibility of creating personalized therapeutic agents towards CRC while in compliance with green chemistry and sustainability metrics.

CRediT authorship contribution statement

Filipe Oliveira: Writing – original draft, Methodology, Funding acquisition, Data curation, Conceptualization. **Joana Pinto:** Writing – original draft, Methodology, Data curation. **Filipa Amaro:** Writing – original draft, Methodology. **Joana Pereira:** Writing – original draft, Methodology. **Inês Ferreira:** Methodology, Data curation. **Mário S. Diniz:** Writing – review & editing, Supervision. **Paula Guedes de Pinho:** Writing – review & editing, Supervision, Funding acquisition. **Ana Rita C. Duarte:** Writing – review & editing, Supervision, Funding acquisition, Conceptualization.

Data availability

The datasets used and/or analyzed during the current study are available from the corresponding author on reasonable request.

Declaration of competing interest

Ana Rita C. Duarte reports a relationship with DES Solutio, Lda that includes: equity or stocks. Ana Rita C. Duarte has patent Terpene based therapeutic deep eutectic solvent, method of obtaining and uses thereof pending to Universidade Nova de Lisboa. If there are other authors, they declare that they have no known competing financial interests or personal relationships that could have appeared to influence the work reported in this paper.

Acknowledgements

This work has received funding from the ERC-2016-CoG 725034 and was supported by the Associate Laboratory for Green Chemistry (LAQV) financed by national funds from FCT/MCTES (UIDP/50006/2020 DOI 10.54499/UIDP/50006/2020). Furthermore, this work received support and help from FCT/MCTES (LA/P/0008/2020 DOI 10.54499/LA/P/0008/2020, UIDP/50006/2020 DOI 10.54499/UIDP/50006/2020 and UIDB/50006/2020 DOI 10.54499/UIDB/50006/2020). The authors acknowledge Fundação para a Ciência e Tecnologia through Filipe Oliveira's PhD grant (2021.07780.BD) and Filipa Amaro's PhD grant (UI/BD/151313/2021). This work was also financed by national funds from Fundação para a Ciência e a Tecnologia. I.P. under the scope of UIDP/04378/2020 and UIDB/04378/2020 projects of the Research Unit on Applied Molecular Biosciences (UCIBIO) and the project LA/P/0140/2020 of the Associate Laboratory Institute for Health and Bioeconomy—i4HB.

Appendix A. Supplementary data

Supplementary data to this article can be found online at https://doi.org/10.1016/j.scp.2025.102037.

Data availability

Data will be made available on request.

References

Abbott, A.P., Capper, G., Davies, D.L., Rasheed, R.K., Tambyrajah, V., 2003. Novel solvent properties of choline chloride/urea mixtures. Chem. Commun. https://doi.org/10.1039/b210714g.
Anastas, P.T., Warner, J.C., 1998. Green Chemistry: Theory and Practice. Oxford University Press.
Apple, G. Long, Lundsmith, E.T., Hamilton, K.E., 2016. Inflammation and colorectal cancer. Curr. Colorectal Cancer Rep. https://doi.org/10.1007/s11888-017-0373-6.
Araújo, A.M., et al., 2018. Analysis of extracellular metabolome by HS-SPME/GC–MS: optimization and application in a pilot study to evaluate galactosamine-induced hepatotoxicity. Toxicol. Lett. https://doi.org/10.1016/J.TOXLET.2018.05.028.
Aroso, I.M., et al., 2015. Design of controlled release systems for THEDES - therapeutic deep eutectic solvents, using supercritical fluid technology. Int. J. Pharm. https://doi.org/10.1016/j.ijpharm.2015.06.038.
Ascar, L., Ahumada, I., López, A., Quintanilla, F., Leiva, K., 2013. Nonsteroidal anti-inflammatory drug determination in water samples by HPLC-DAD under isocratic conditions. J. Braz. Chem. Soc. https://doi.org/10.5935/0103-5053.20130150.
Aylaz, G., et al., 2021. Quality of life after colorectal surgery: a prospective study of patients compared with their spouses. World J. Gastrointest. Surg. https://doi.org/10.4240/WJGS.V13.I9.1050.
Baars, J.E., et al., 2012. Age at diagnosis of inflammatory bowel disease influences early development of colorectal cancer in inflammatory bowel disease patients: a nationwide, long-term survey. J. Gastroenterol. https://doi.org/10.1007/S00535-012-0603-2/FIGURES/4.
Beliaeff, B., Burgeot, T., 2002. Integrated biomarker response: a useful tool for ecological risk assessment. Environ. Toxicol. Chem. https://doi.org/10.1002/ETC.5620210629.
Berben, L., Sereika, S.M., Engberg, S., 2012. Effect size estimation: methods and examples. Int. J. Nurs. Stud. https://doi.org/10.1016/J.IJNURSTU.2012.01.015.
Bradford, M.M., 1976. A rapid and sensitive method for the quantitation of microgram quantities of protein utilizing the principle of protein-dye binding. Anal. Biochem. https://doi.org/10.1016/0003-2697(76)90527-3.
Bray, F., et al., 2024. Global cancer statistics 2022: GLOBOCAN estimates of incidence and mortality worldwide for 36 cancers in 185 countries. CA Cancer J. Clin. https://doi.org/10.3322/caac.21834.
Bridges, D., Saltiel, A.R., 2012. Phosphoinositides and disease. Curr. Top. Microbiol. Immuno.
Byun, H.K., Koom, W.S., 2023. A practical review of watch-and-wait approach in rectal cancer. Radiat. Oncol. J. https://doi.org/10.3857/ROJ.2023.00038.
Calder, P.C., 2015. Functional roles of fatty acids and their effects on human Health. J. Parenter. Enter. Nutr. https://doi.org/10.1177/0148607115595980.
Cheng, Y., Ling, Z., Li, L., 2020. The intestinal microbiota and colorectal cancer. Front. Immunol. https://doi.org/10.3389/FIMMU.2020.615056.
Chu, L.Y., Li, Y., Zhu, J.H., Wang, H.D., Liang, Y.J., 2004. Control of pore size and permeability of a glucose-responsive gating membrane for insulin delivery. J. Control. Release. https://doi.org/10.1016/J.JCONREL.2004.02.026.
Coussens, L.M., Werb, Z., 2002. Inflammation and cancer. Nature. https://doi.org/10.1038/NATURE01322.
Cruz, J.P.C., et al., 2023. Short-term biochemical biomarkers of stress in the oyster magallana angulata exposed to gymnodinium catenatum and skeletonema marinoi. Science. https://doi.org/10.3390/SCI5030030.
Cucchi, D., et al., 2020. Fatty acids - from energy substrates to key regulators of cell survival, proliferation and effector function. Cell Stress. https://doi.org/10.15698/CST2020.01.209.
DeBerardinis, R.J., Chandel, N.S., 2020. We need to talk about the Warburg effect. Nat. Metab. 22 (2020). https://doi.org/10.1038/s42255-020-0172-2.

Devin, S., Burgeot, T., Giambérini, L., Minguez, L., Pain-Devin, S., 2014. The integrated biomarker response revisited: optimization to avoid misuse. Environ. Sci. Pollut. Res. https://doi.org/10.1007/s11356-013-2169-9.
Duarte, A.R.C., et al., 2017. A comparison between pure active pharmaceutical ingredients and therapeutic deep eutectic solvents: solubility and permeability studies. Eur. J. Pharm. Biopharm. https://doi.org/10.1016/j.ejpb.2017.02.003.
Dueck, D.A., et al., 1996. The modulation of choline phosphoglyceride metabolism in human colon cancer. Mol. Cell. Biochem. https://doi.org/10.1007/BF00227535/METRICS.
Duelund, L., Amiot, A., Fillon, A., Mouritsen, O.G., 2012. Influence of the active compounds of Perilla frutescens leaves on lipid membranes. J. Nat. Prod. https://doi.org/10.1021/NP200713Q/SUPPL_FILE/NP200713Q_SI_001. PDF.
Edelblum, K.L., Turner, J.R., 2015. Epithelial cells: structure, transport, and barrier function. Mucosal Immunol. https://doi.org/10.1016/B978-0-12-415847-4.00012-4. Fourth Ed.
Elsisi, N.S., Darling-Reed, S., Lee, E.Y., Oriaku, E.T., Soliman, K.F., 2005. Ibuprofen and apigenin induce apoptosis and cell cycle arrest in activated microglia. Neurosci. Lett. https://doi.org/10.1016/J.NEULET.2004.10.087.
Farrugia, G., Balzan, R., 2013. The proapoptotic effect of traditional and novel nonsteroidal anti-inflammatory drugs in mammalian and yeast cells. Oxid. Med. Cell. Longev. https://doi.org/10.1155/2013/504230.
Ferreira, I.J., Meneses, L., Paiva, A., Diniz, M., Duarte, A.R.C., 2022. Assessment of deep eutectic solvents toxicity in zebrafish (Danio rerio). Chemosphere. https://doi.org/10.1016/j.chemosphere.2022.134415.
Figueiredo, C., et al., 2020. Warming enhances lanthanum accumulation and toxicity promoting cellular damage in glass eels (Anguilla anguilla). Environ. Res. https://doi.org/10.1016/J.ENVRES.2020.110051.
Gerbig, S., et al., 2012. Analysis of colorectal adenocarcinoma tissue by desorption electrospray ionization mass spectrometric imaging. Anal. Bioanal. Chem. https://doi.org/10.1007/S00216-012-5841-X/METRICS.
Gillaspy, G.E., 2011. The cellular language of myo-inositol signaling. New Phytol. https://doi.org/10.1111/J.1469-8137.2011.03939.X.
Greenspan, E.J., Madigan, J.P., Boardman, L.A., Rosenberg, D.W., 2011. Ibuprofen inhibits activation of nuclear beta-catenin in human colon adenomas and induces the phosphorylation of GSK-3(beta). Cancer Prev. Res. https://doi.org/10.1158/1940-6207.CAPR-10-0021.
Guittin, C., et al., 2023. New online monitoring approaches to describe and understand the kinetics of acetaldehyde concentration during wine alcoholic fermentation: access to production balances. Fermentation. https://doi.org/10.3390/fermentation9030299.
Hanahan, D., 2022. Hallmarks of cancer: new dimensions. Cancer Discov. https://doi.org/10.1158/2159-8290.CD-21-1059.
Hansen, B.B., et al., 2021. Deep eutectic solvents: a review of fundamentals and applications. Chem. Rev. https://doi.org/10.1021/acs.chemrev.0c00385.
Hayyan, M., Looi, C.Y., Hayyan, A., Wong, W.F., Hashim, M.A., 2015. In Vitro and in Vivo toxicity profiling of ammonium-based deep eutectic solvents. PLoS One. https://doi.org/10.1371/journal.pone.0117934.
Heinlein, A., Metzger, M., Walles, H., Buettner, A., 2014. Transport of hop aroma compounds across Caco-2 monolayers. Food Funct. https://doi.org/10.1039/C3FO60675A.
Hnatyszyn, A., et al., 2019. Colorectal carcinoma in the course of inflammatory bowel diseases. Hered. Cancer Clin. Pract. https://doi.org/10.1186/S13053-019-0118-4/TABLES/1.
Huang, H., et al., 2019. Inhibition of PGE 2/EP4 receptor signaling enhances oxaliplatin efficacy in resistant colon cancer cells through modulation of oxidative stress. Sci. Rep. https://doi.org/10.1038/S41598-019-40848-4.
Jewison, T., et al., 2014. Smpdb 2.0: big improvements to the small molecule pathway database. Nucleic Acids Res. https://doi.org/10.1093/NAR/GKT1067.
Kanehisa, M., Furumichi, M., Sato, Y., Kawashima, M., Ishiguro-Watanabe, M., 2023. KEGG for taxonomy-based analysis of pathways and genomes. Nucleic Acids Res. https://doi.org/10.1093/NAR/GKAC963.
Kehrer, J.P., Robertson, J.D., Smith, C.V., 2010. Free radicals and reactive oxygen species. In: Comprehensive Toxicology, second ed. https://doi.org/10.1016/B978-0-08-046884-6.00114-7
Kumar, A., et al., 2023. Current and emerging therapeutic approaches for colorectal cancer: a comprehensive review. World J. Gastrointest. Surg. https://doi.org/10.4240/wjgs.v15.i4.495.
Ladabaum, U., Dominitz, J.A., Kahi, C., Schoen, R.E., 2020. Strategies for colorectal cancer screening. Gastroenterology. https://doi.org/10.1053/J.GASTRO.2019.06.043.
Lam, C.H., Escande, V., Mellor, K.E., Zimmerman, J.B., Anastas, P.T., 2019. Teaching atom economy and E-factor concepts through a green laboratory experiment: aerobic oxidative cleavage of meso-hydrobenzoin to benzaldehyde using a heterogeneous catalyst. J. Chem. Educ. https://doi.org/10.1021/acs.jchemed.8b00058.
Lam, G., et al., 2023. The effects of pollutant mixture released from grafted adipose tissues on fatty acid and lipid metabolism in the skeletal muscles, kidney, heart, and lungs of male mice. Environ. Pollut. https://doi.org/10.1016/j.envpol.2023.122387.
Leone, A., et al., 2021. The dual-role of methylglyoxal in tumor progression – novel therapeutic approaches. Front. Oncol. https://doi.org/10.3389/fonc.2021.645686.
Leong, K.H., et al., 2016. Cycloart-24-ene-26-ol-3-one, a new cycloartane isolated from leaves of Aglaia exima triggers tumour necrosis factor-receptor 1-mediated caspase-dependent apoptosis in colon cancer cell line. PLoS One. https://doi.org/10.1371/journal.pone.0152652.
Levi, L., Wang, Z., Doud, M.K., Hazen, S.L., Noy, N., 2015. Saturated fatty acids regulate retinoic acid signalling and suppress tumorigenesis by targeting fatty acid-binding protein 5. Nat. Commun. https://doi.org/10.1038/NCOMMS9794.
Lima, A.R., et al., 2018a. Discrimination between the human prostate normal and cancer cell exometabolome by GC-MS. Sci. Rep. https://doi.org/10.1038/s41598-018-23847-9.
Lima, A.R., et al., 2018b. GC-MS-based endometabolome analysis differentiates prostate cancer from normal prostate cells. Metabolites. https://doi.org/10.3390/metabo8010023.
Lin, S., Li, Y., Zamyatnin, A.A., Werner, J., Bazhin, A.V., 2018. Reactive oxygen species and colorectal cancer. J. Cell. Physiol. https://doi.org/10.1002/JCP.26356.
Lopes, A.R., et al., 2018. Absence of cellular damage in tropical newly hatched sharks (Chiloscyllium plagiosum) under ocean acidification conditions. Cell Stress Chaperones. https://doi.org/10.1007/S12192-018-0892-3.
Mbous, Y.P., Hayyan, M., Wong, W.F., Looi, C.Y., Hashim, M.A., 2017. Unraveling the cytotoxicity and metabolic pathways of binary natural deep eutectic solvent systems. Sci. Rep. https://doi.org/10.1038/srep41257.
Mbous, Y.P., et al., 2020. Simulation of deep eutectic solvents' interaction with membranes of cancer cells using COSMO-RS. J. Phys. Chem. B. https://doi.org/10.1021/acs.jpcb.0c04801.
McGleenon, B.M., Dynan, K.B., Passmore, A.P., 1999. Acetylcholinesterase inhibitors in Alzheimer's disease. Br. J. Clin. Pharmacol. https://doi.org/10.1046/J.1365-2125.1999.00026.X.
Melo, J.B., Agostinho, P., Oliveira, C.R., 2003. Involvement of oxidative stress in the enhancement of acetylcholinesterase activity induced by amyloid beta-peptide. Neurosci. Res. https://doi.org/10.1016/S0168-0102(02)00201-8.
Mladenović, M., et al., 2018. The targeted pesticides as acetylcholinesterase inhibitors: comprehensive cross-organism molecular modelling studies performed to anticipate the pharmacology of harmfulness to humans in vitro. Mol. A J. Synth. Chem. Nat. Prod. Chem. https://doi.org/10.3390/MOLECULES23092192.
Nakaweh, A., Al-Akayleh, F., Al-Remawi, M., Abdallah, Q., Agha, A.S.A.A., 2024. Deep eutectic system-based liquisolid nanoparticles as drug delivery system of curcumin for in-vitro colon cancer cells. J. Pharm. Innov. https://doi.org/10.1007/s12247-024-09826-w.
Nascimento, A.L.C.S., et al., 2021. Co-crystals of non-steroidal anti-inflammatory drugs (NSAIDs): insight toward formation, methods, and drug enhancement. Particuology. https://doi.org/10.1016/J.PARTIC.2021.03.015.
Ogunrinola, G.A., Oyewale, J.O., Oshamika, O.O., Olasehinde, G.I., 2020. The human microbiome and its impacts on Health. Int. J. Microbiol. https://doi.org/10.1155/2020/8045646.

Oliveira, F. S. N. de, Duarte, A.R.C., 2021. A look on target-specificity of eutectic systems based on natural bioactive compounds. In: Advances in Botanical Research. https://doi.org/10.1016/bs.abr.2020.09.008.
Oliveira, F., et al., 2023. Menthol-based deep eutectic systems as antimicrobial and anti-inflammatory agents for wound healing. Eur. J. Pharm. Sci. https://doi.org/10.1016/j.ejps.2022.106368.
Omkvist, D.H., Brodin, B., Nielsen, C.U., 2010. Ibuprofen is a non-competitive inhibitor of the peptide transporter hPEPT1 (SLC15A1): possible interactions between hPEPT1 substrates and ibuprofen. Br. J. Pharmacol. https://doi.org/10.1111/J.1476-5381.2010.01000.X.
Pang, Z., et al., 2021. MetaboAnalyst 5.0: narrowing the gap between raw spectra and functional insights. Nucleic Acids Res. https://doi.org/10.1093/NAR/GKAB382.
Pei, J., Pan, X., Wei, G., Hua, Y., 2023. Research progress of glutathione peroxidase family (GPX) in redoxidation. Front. Pharmacol. https://doi.org/10.3389/FPHAR.2023.1147414.
Pereira, C.V., et al., 2019. Unveil the anticancer potential of limomene based therapeutic deep eutectic solvents. Nat. Sci. Reports. https://doi.org/10.1038/s41598-019-51472-7.
Pereira, J., et al., 2022. Selective terpene based therapeutic deep eutectic systems against colorectal cancer. Eur. J. Pharm. Biopharm. https://doi.org/10.1016/j.ejpb.2022.04.008.
Pluskal, T., Castillo, S., Villar-Briones, A., Orešič, M., 2010. MZmine 2: modular framework for processing, visualizing, and analyzing mass spectrometry-based molecular profile data. BMC Bioinf. https://doi.org/10.1186/1471-2105-11-395.
Radošević, K., et al., 2018. Antimicrobial, cytotoxic and antioxidative evaluation of natural deep eutectic solvents. Environ. Sci. Pollut. Res. https://doi.org/10.1007/s11356-018-1669-z.
Reiffen, K.A., Schneider, F., 1984. A comparative study on proliferation, macromolecular synthesis and energy metabolism of in vitro-grown Ehrlich ascites tumor cells in the presence of glucosone, galactosone and methylglyoxal. J. Cancer Res. Clin. Oncol. https://doi.org/10.1007/BF01032608.
Rizzo, W.B., et al., 2008. Abnormal fatty alcohol metabolism in cultured keratinocytes from patients with Sjögren-Larsson syndrome William. J. Lipid Res. https://doi.org/10.1194/jlr.M700469-JLR200.
Rodriguez, F.D., Coveñas, R., 2021. Biochemical mechanisms associating alcohol use disorders with cancers. Cancers (Basel). https://doi.org/10.3390/cancers13143548.
Rtibi, K., Marzouki, L., Sebai, H., 2021. Oxidative stress due to 5-fluorouracil and dietary antioxidants. Toxicol. Oxidative Stress Diet. Antioxidants. https://doi.org/10.1016/B978-0-12-819092-0.00028-5.
Sambuy, Y., et al., 2005. The Caco-2 cell line as a model of the intestinal barrier: influence of cell and culture-related factors on Caco-2 cell functional characteristics. Cell Biol. Toxicol. https://doi.org/10.1007/s10565-005-0085-6.
Santos, F., Duarte, A.R.C., 2021. Therapeutic Deep Eutectic Systems for the Enhancement of Drug Bioavailability, vol. 9. https://doi.org/10.1007/978-3-030-53069-3_3.
Santos, F., Leitão, M.I.P.S., Duarte, A.R.C., 2019. Properties of therapeutic deep eutectic solvents of L-arginine and ethambutol for tuberculosis treatment. Molecules. https://doi.org/10.3390/molecules24010055.
Santos, F., Pires, D., Anes, E., Rita, A., Duarte, C., 2023. Insights into therapeutic liquid mixtures and formulations towards tuberculosis therapy. Int. J. Pharm. https://doi.org/10.1016/j.ijpharm.2023.122862.
Sheldon, R.A., 2017. The: E factor 25 years on: the rise of green chemistry and sustainability. Green Chem. https://doi.org/10.1039/c6gc02157c.
Silva, J.M., et al., 2014. Tailored freestanding multilayered membranes based on chitosan and alginate. Biomacromolecules. https://doi.org/10.1021/BM501156V/SUPPL_FILE/BM501156V_SI_001. PDF.
Silva, E., et al., 2020. Optimal design of thedes based on perillyl alcohol and ibuprofen. Pharmaceutics. https://doi.org/10.3390/pharmaceutics12111121.
Silva, E., Oliveira, F., Silva, J.M., Reis, R.L., Duarte, A.R.C., 2021. Untangling the bioactive properties of therapeutic deep eutectic solvents based on natural terpenes. Curr. Res. Chem. Biol. https://doi.org/10.1016/j.crchbi.2021.100003.
Sung, H., et al., 2025. Colorectal cancer incidence trends in younger versus older adults: an analysis of population-based cancer registry data. Lancet Oncol. https://doi.org/10.1016/S1470-2045(24)00600-4.
Tan, J., et al., 2015. Genetic variants in the inositol phosphate metabolism pathway and risk of different types of cancer. Sci. Rep. https://doi.org/10.1038/srep08473.
Thornalley, P.J., Langborg, A., Minhas, H.S., 1999. Formation of glyoxal, methylglyoxal and 3-deoxyglucosone in the glycation of proteins by glucose. Biochem. J. https://doi.org/10.1042/0264-6021:3440109.
Tsuchida, S., 2002. Glutathione transferases. In: Encyclopedia of Cancer. https://doi.org/10.1016/B0-12-227555-1/00513-X.
Tsukagoshi, S., Lembach, K., Charalampous, F.C., 1966. Metabolic functions of myo-inositol. J. Biol. Chem. https://doi.org/10.1016/S0021-9258(18)96929-2.
United Nations, 2016. Transforming Our World: the 2030 Agenda for Sustainable Development.
Valente, S., et al., 2023. Hydrophobic DES based on menthol and natural organic acids for use in antifouling marine coatings. ACS Sustain. Chem. Eng. https://doi.org/10.1021/acssuschemeng.3c01120.
Wikene, K.O., Rukke, H.V., Bruzell, E., Tønnesen, H.H., 2017. Investigation of the antimicrobial effect of natural deep eutectic solvents (NADES) as solvents in antimicrobial photodynamic therapy. J. Photochem. Photobiol., A. https://doi.org/10.1016/j.jphotobiol.2017.04.030.
Wishart, D.S., 2016. Emerging applications of metabolomics in drug discovery and precision medicine. Nat. Rev. Drug Discov. https://doi.org/10.1038/NRD.2016.32.
Yang, H., Dou, Q.P., 2010. Targeting apoptosis pathway with natural terpenoids: implications for treatment of breast and prostate cancer. Curr. Drug Targets. https://doi.org/10.2174/138945010791170842.
Zainal-Abidin, M.H., Hayyan, M., Ngoh, G.C., Wong, W.F., Looi, C.Y., 2019. Emerging frontiers of deep eutectic solvents in drug discovery and drug delivery systems. J. Control. Release. https://doi.org/10.1016/j.jconrel.2019.09.019.
Zakrewsky, M., et al., 2016. Choline and geranate deep eutectic solvent as a broad-spectrum antiseptic agent for preventive and therapeutic applications. Adv. Healthc. Mater. https://doi.org/10.1002/adhm.201600086.
Zappavigna, S., et al., 2020. Anti-inflammatory drugs as anticancer agents. Int. J. Mol. Sci. https://doi.org/10.3390/IJMS21072605.
Zhang, Q., De Oliveira Vigier, K., Royer, S., Jérôme, F., 2012. Deep eutectic solvents: syntheses, properties and applications. Chem. Soc. Rev. https://doi.org/10.1039/C2CS35178A.